



ÉCOLE  
POLYTECHNIQUE  
DE BRUXELLES



UNIVERSITÉ LIBRE DE BRUXELLES

# Development of an open access software for the design and the implementation of solar dryers within developing country cooperatives

Mémoire présenté en vue de l'obtention du diplôme  
d'Ingénieur Civil en informatique à finalité spécialisée

**Lucie Cuvelliez Drowart**

Directeur

Professeur Benoît Haut

Co-Promoteur

Ir. Cédric Boey

Service

Travail réalisé au service TIPs

Année académique

2020 - 2021

## Acknowledgements

I would like first to deeply thank Benoit Haut and Cedric Boey for having been very present supervisors, who were available at all times whenever I had a doubt or a question. I would also thank Benoit Haut for the long hours he took to comment on the present text in order to make it reasonably good.

Special thanks to my friends Quentin and Boris for their support and for always reminding me that no thing should be apprehended too seriously.

Finally, I am very grateful to my father, who carefully read and commented this master thesis, and my mother for the opportunity to carry these studies and her relentless support over the years.

## Abstract

### **Development of an open access software for the design and the implementation of solar dryers within developing country cooperatives**

Lucie Cuvellez Drowart

Master en Ingénieur Civil en informatique à finalité spécialisée  
2020-2021

Au sein des communautés de petits agriculteurs des pays en voie de développement, le séchage alimentaire est encore souvent réalisé à l'air libre, entraînant, entre autres, de nombreuses pertes dues aux intempéries et un séchage parfois inhomogène. De simples séchoirs solaires peuvent améliorer la qualité et le rendement du séchage, sans pour autant nécessiter des coûts importants supplémentaires. Ces technologies ne sont cependant pas encore adoptées par les communautés locales. L'une des raisons en est le manque d'une procédure de conception facilement accessible à un utilisateur non expert. En conséquence, ce travail a pour but la création d'un site web dédié au dimensionnement d'un séchoir solaire de type tunnel fonctionnant en ventilation forcée. Dans ce type de séchoir, un panneau solaire alimente des ventilateurs, qui génèrent donc un écoulement d'air. Le séchoir est composé d'une zone de chauffe et d'une zone de séchage. Dans la zone de chauffe, il n'y a pas de produits à sécher. En avançant dans la zone de chauffe, l'air voit sa température augmenter grâce à l'effet de serre. Dans la zone de séchage, les produits à sécher sont disposés en tranches. Les produits sont en contact avec l'air préalablement chauffé et soumis à un rayonnement solaire. Ainsi, l'eau contenue dans les produits s'évapore et la vapeur d'eau produite est évacuée de l'appareil avec l'air le quittant. Nous proposons une procédure de dimensionnement basée sur des équations de bilan d'énergie et de masse. Cette procédure permet de concevoir le système de ventilation et de calculer les longueurs de la zone de chauffe et de la zone de séchage du séchoir selon un cahier des charges défini par l'utilisateur et selon des conditions de conception qui assurent un séchage efficace et homogène. L'encodage du cahier des charges et les résultats du dimensionnement sont facilement accessibles à l'utilisateur via un site web basé sur le framework Flask. Bien qu'il nécessite encore des améliorations d'ordre fonctionnel et esthétique, notre site web remplit sa fonction première et permet à un utilisateur qui n'est pas nécessairement un expert en séchage de dimensionner rapidement un simple séchoir solaire pouvant sécher une vingtaine de kilo de produit.

**Mots clés :** séchage alimentaire, séchoir solaire, procédure de dimensionnement, interface utilisateur

# Contents

<b>1</b>	<b>Introduction</b>	<b>1</b>
1.1	Purpose . . . . .	1
1.2	Problem statement . . . . .	2
1.3	Choice of the design of the drying technology . . . . .	2
1.3.1	Flow motion . . . . .	3
1.3.2	Air heating mode . . . . .	3
1.3.3	Box-type, cabinet and tunnel solar dryer . . . . .	5
1.3.4	Description of the dryer considered in this work . . . . .	6
<b>2</b>	<b>Model and design procedure</b>	<b>7</b>
2.1	Introduction . . . . .	7
2.2	Main parameters involved in the design procedure . . . . .	7
2.2.1	Climatic data . . . . .	7
2.2.2	Product specifications . . . . .	7
2.2.3	Geometry of the dryer . . . . .	9
2.3	Assumptions and design condition . . . . .	9
2.3.1	Assumptions . . . . .	9
2.3.2	Design conditions . . . . .	10
2.4	Design of the dryer . . . . .	11
2.4.1	Design of the ventilation system . . . . .	11
2.4.2	Design of the heating and the drying parts . . . . .	12
2.5	Numerical resolution . . . . .	17
2.6	Results of the design procedure for two situations . . . . .	18
2.6.1	Cambodia . . . . .	19
2.6.2	Uganda . . . . .	20
<b>3</b>	<b>Open access software</b>	<b>22</b>
3.1	Introduction . . . . .	22
3.2	Choice between desktop and web application . . . . .	22
3.3	Flask framework . . . . .	23
3.4	Structure of the application . . . . .	23
3.5	User journey . . . . .	25
3.5.1	Home page . . . . .	25
3.5.2	Design your solar dryer page . . . . .	25
3.5.3	Contacts page . . . . .	28
3.5.4	About page . . . . .	28
3.6	Web hosting . . . . .	28
<b>4</b>	<b>Future work</b>	<b>29</b>
4.1	Introduction . . . . .	29
4.2	Model . . . . .	29
4.2.1	Experimental tests . . . . .	29
4.2.2	Sensitivity analysis of the parameters . . . . .	29
4.3	Website . . . . .	30
4.3.1	Explanations and resources for the input parameters . . . . .	30
4.3.2	User session . . . . .	30

<b>5</b>	<b>Conclusions</b>	<b>31</b>
<b>A</b>	<b>Drying time of different fruits for several slice thicknesses and drying temperatures</b>	<b>32</b>
<b>B</b>	<b>Conditions on user inputs in the website</b>	<b>33</b>

# List of Figures

1.1	Sun drying of sliced tomatoes on drying racks [3] . . . . .	1
1.2	Classification of solar dryers and drying modes [11] . . . . .	3
1.3	Example of an active direct sun dryer. Black arrows represent the air flow, white arrows represent the solar radiation flux [13] . . . . .	4
1.4	Example of an active indirect sun dryer [13] . . . . .	4
1.5	Example of an active mixed mode sun dryer [13] . . . . .	4
1.6	Schematic of a box-type solar dryer (direct) [16] . . . . .	5
1.7	Sectional view of a cabinet solar dryer (mixed mode) [17] . . . . .	5
1.8	Schematic of a tunnel solar dryer [18] . . . . .	5
1.9	Schematic drawing of a ventilated tunnel solar dryer (adapted from [6]): (1) fans, (2) photovoltaic module, (3) transparent plastic sheet, (4) black matte floor, (5) tray with products to dry, (6) heating part, (7) drying part . . . . .	6
2.1	Schematic flow cross section of the dryer designed . . . . .	9
2.2	Air flow in the solar tunnel dryer. The design conditions impose that, on average, the air leaving the heating zone is at temperature $T_d$ and that, on average, the air temperature at the end of the drying zone is $T_d$ as well. . . . .	10
2.3	Energy fluxes (in $\text{W}/\text{m}^2$ ) represented in a transversal cut of the (a) heating zone (b) drying zone. The 3 gray rectangles delimit the zones selected to express the energy balance equations . . . . .	12
2.4	Schematic of a product slice . . . . .	16
2.5	Schematic top view of the products disposed on the floor . . . . .	16
2.6	Temperature of the air $T_{\text{air}}$ at the end of the heating section for $L_H = 2.2$ m with the scope statement of Cambodia. The starting drying time is 09:45 am and total drying time is 6.5h. The mean temperature of the air at the end of the heating section is $62.8^\circ\text{C}$ . . . . .	19
2.7	Energy flux transferred to the air inside the dryer $P$ at the end of the heating section for $L_H = 2.2$ m with the scope statement of Cambodia. The mean value of $P$ is $147.3 \text{ W}/\text{m}^2$ . . . . .	19
2.8	Drying rate $J$ with the scope statement of Cambodia. The mean drying rate is 1.06 kg of water evaporated per hour and per kg of dry product . . . . .	20
2.9	Temperature of the air $T_{\text{air}}$ at the end of the heating section for $L_H = 2.3$ m with the scope statement of Uganda. The starting drying time is 08:00 am and total drying time is 8h. The mean temperature of the air at the end of the heating section is $70.4^\circ\text{C}$ . . . . .	20
2.10	Energy flux transferred to the air inside the dryer $P$ at the end of the heating section for $L_H = 2.3$ m with the scope statement of Uganda. The mean value is $159.6 \text{ W}/\text{m}^2$ . . . . .	21
2.11	Drying rate $J$ with the scope statement of Uganda. The mean drying rate is 0.68 kg of water evaporated per hour and per kg of dry product . . . . .	21
3.1	Client-server communication through HTTP [34] . . . . .	24
3.2	Home page of <i>Dreasy</i> . . . . .	25
3.3	Calculating the air flow rate required, the user is invited to enter climatic data and product specifications . . . . .	25
3.4	Database of the drying time for different fruits at different drying temperature and slice thicknesses . . . . .	26
3.5	Example of warnings appearing when the user enters incoherent values . . . . .	26

3.6	Ventilation system information are displayed to the user . . . . .	27
3.7	Calculating the lengths of the heating and drying zone. Parameters entered previously are displayed but the user is not allowed to change them at this stage . . . .	27
3.8	Starting time and lengths of the heating and drying sections are displayed. A schematic flow cross section with the dimensions is also displayed . . . . .	28
3.9	Contacts page . . . . .	28

# List of Tables

2.1	Data to collect before starting the design procedure . . . . .	8
2.2	Scope statement and data collected of the dryers built in Cambodia and in Uganda. Climatic data come from online resources and measurements on the field [6] . . . .	18
2.3	Results of the design procedure . . . . .	18
3.1	Comparison between desktop application and web application on several aspects. Adapted from [30] . . . . .	23
A.1	Drying time of different fruits for several slice thicknesses and drying temperatures, obtained experimentally. Products are dried from their initial humidity to a final humidity of 0.05 kg water/kg dry product. . . . .	32
B.1	Conditions on user inputs in the website . . . . .	33



# List of symbols

Symbol	Description	Units
<i>Roman symbols</i>		
$C$	Convective heat flux	W/m <sup>2</sup>
$C$	Heat capacity	J/kg/K
$D$	Conductive heat flux	W/m <sup>2</sup>
$E$	Activation energy	J/mol
$F$	Design coefficient	–
$g$	Standard gravity	m/s <sup>2</sup>
Gr	Grashof number	–
$h$	Convective heat transfer coefficient	W/m <sup>2</sup> K
$I$	Infrared radiation flux	W/m <sup>2</sup>
$J$	Drying rate	kg water/kg dry product/s
$k$	Reduction factor	–
$L$	Length	m
$\mathcal{L}$	Mass latent heat of vaporization	J/kg
$M$	Mass of product	kg
$\widehat{M}$	Molar mass	kg/mol
Nu	Nusselt number	–
Pr	Prandtl number	–
$P$	Energy flux transferred to the air inside the dryer	W/m <sup>2</sup>
$p$	Pressure	Pa
$Q$	Air flow rate	kg humid air/s
$R$	Aspect ratio	–
Ra	Rayleigh number	–
RH	Relative humidity	%
$R_g$	Molar gas constant	J/mol K
$S$	Direct and diffuse solar radiation flux	W/m <sup>2</sup>
$t$	Time	s
$T$	Temperature	K
$W_d$	Width of the dryer	m
$W_p$	Length of the cross section of the plastic cover transverse to the flow	m
$X$	Moisture content of product	kg water/kg dry product

Symbol	Description	Units
$Y$	Air humidity	kg water/kg dry air
$z$	longitudinal position in the dryer	m
<i>Greek symbols</i>		
$\beta$	Thermal expansion coefficient	1/K
$\epsilon$	Emissivity	–
$\lambda$	Thermal conductivity	W/m/K
$\nu$	Kinematic viscosity	m <sup>2</sup> /s
$\rho$	Density	kg/m <sup>3</sup>
$\sigma$	Stefan–Boltzmann constant	W/m <sup>2</sup> /K
<i>Subscripts</i>		
0	Initial	
a	Air	
air	Air inside the dryer	
amb	Ambient air	
atm	Atmospheric	
c	Characteristic	
d	Drying	
D	Drying part	
f	Final	
fl	Floor	
H	Heating part	
m	Diurnal mean	
max	Maximal	
min	Minimal	
p	Plastic	
rise	Sunrise	
s	Surface	
sat	Saturation	
set	Sunset	
w	Water	

# Chapter 1

## Introduction

### 1.1 Purpose

Drying is the process of reducing the moisture content of food products. Drying is also an effective food preservation technique. The dehydrated products are less likely to spoil because removing water inhibits the growth of bacteria, mold and yeast. Apart from food preservation, another advantage of drying is that it reduces the product volume and weight. Hence, it allows a compact storage. Products are easy to store and pack, and it reduces the price of transportation. Because of all those advantages, drying is widely used in the food industry [1].

A large number of drying techniques exist. The optimal method depends on many factors such as the type of product to dry, the quantity, the climatic conditions or the economic investment. Sun drying, also called open-air drying, is the easiest and cheapest solar drying technique. The products are simply laid down in trays or on the ground and directly exposed in the sun (Fig. 1.1). Even though it is easy to implement and almost without costs, open air drying is a risky process and presents many downsides. The products are not protected from the dust nor weather-proof. The drying is fully dependent of the weather: sudden rains can ruin several hours of drying. There is also a risk of mould growth. It is difficult to control the drying temperature, leading to inhomogeneous and low quality dried product. In addition, the drying rate of open-air drying is relatively slow compared to other drying methods [2].



Figure 1.1: Sun drying of sliced tomatoes on drying racks [3]

Solar drying systems can help to overcome the limitations of open air drying. In such systems, the product is dried in a closed environment where the temperature is higher than the ambient temperature. Typically, solar dryers are composed of three elements: a drying part in which products are dried, a heating part which heats the air using solar energy and some type of air-flow system [4]. The product is heated by the warmed air and sometimes by the solar energy as well.

In developing countries, the majority of the population lives from agriculture production. Despite the disadvantages stated above, many small-scale farmers still dry their product using sun drying. Simple improved solar dryers can be economical and increase farmers income substantially. There has been attempt to implement solar drying systems in the small-scale farmers communities but

such technologies are not yet adopted by local communities. In some cases, the dryers were not able to meet users expectations because their design was based on models which did not reflect the reality. In other cases, technology transfer was the issue: the local communities were not involved in the implementation of the solar dryers. Hence, it was difficult for farmers to uptake knowledge to conduct solar drying and maintain the equipment [5].

Recently, Talbot et al. [6] proposed a systematic procedure to design solar dryers for small-scale farmers communities. The results have been validated through experiments on fresh mango slices in Cambodia and on fresh pineapple slices in Uganda. The design procedure, based on energy and mass balance equations, is thoroughly explained in the paper. However, a repository with the implementation is not provided. Hence, anyone looking to design a dryer based on this procedure would have to solve the equations himself. The user is required to have a high educational level, a tool for numerical calculations and a significant amount of time to spend on the design procedure. In addition, there is no guarantee the user will not miscalculate or misunderstand some parts of the procedure. Finally, small-scale farmers communities may not have access to all the scientific publications needed.

## 1.2 Problem statement

In the light of these considerations, we strongly believe an open-access software to design and implement a simple solar dryer would help small-scale farmers communities to significantly increase their production. In this thesis, we aim at developing a user-friendly software that would help the user to build a solar dryers based on Talbot et al. design procedure. Furthermore, Tabot et al. assume that the evaporation rate inside the dryer is constant, although it is well known that the drying rate of a product is a decreasing function of time [7][8]. We decide to remove this hypothesis and to model the drying rate as varying with time and temperature. This results on a significant impact on the dimensions of the dryer.

According to specifications defined by the user, our software returns the optimal dimensions of the dryer to obtain an homogeneous drying. We have defined users as educated people who do not necessarily have drying expertise but are used to do research and have intermediate level of knowledge. The user must be able to carry out steps on the basis of instructions (e.g. determine the quantity of water contained in a product). Targeted users are, for example, managers of developing country cooperatives.

This thesis is divided in three parts. In Chapter 2, we define the design procedure of the dryer and its implementation. In Chapter 3, we present the development and interface of our open access software. In Chapter 4, we discuss a list of priorities which will serve as a foundation for further work.

## 1.3 Choice of the design of the drying technology

Users may face several distinct technological options for simple solar drying systems. The purpose of this section is to present a description of the main solar drying technologies and to justify the choice of the most suitable one.

Solar dryers can be classified according to the air heating system and the ventilation system [4] [9]. Fig. 1.2 presents a basic classification of the solar dryers and drying modes. The movement of the air in the dryer can be the result of natural convection or forced convection. Those two groups are respectively named passive dryers and active dryers. All types of natural convection dryers can be operated by forced convection as well [10]. Regarding the air heating system, the air can be directly heated in the food chamber, pre-heated in a solar collector or a mix of the two. Some dryers heat the air using solar energy as well as an another source of energy. Various types of construction are possible, no matter the air heating system. The basic constructions of solar dryers are the box-type dryer, the cabinet dryer and the tunnel dryer (see Section 1.3.3). The

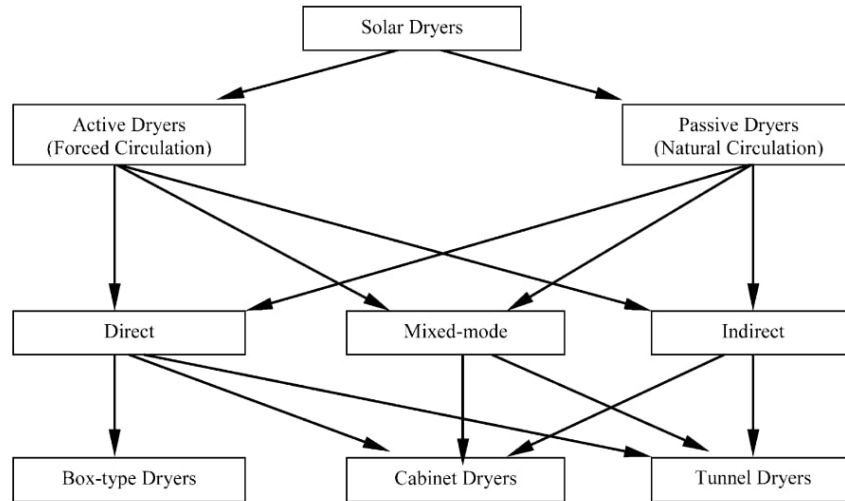


Figure 1.2: Classification of solar dryers and drying modes [11]

dryer chosen should optimize three criteria: (1) it has a good drying performance, (2) it is easy to build and to maintain, (3) it minimizes initial and operating costs.

### 1.3.1 Flow motion

The temperature inside the solar dryer is higher than the ambient temperature outside it. As a result, the water inside the product evaporates. The air inside the dryer can absorb the moisture of the product until a certain equilibrium is reached. A good circulation of the air is crucial for the drying process since it ensures that this air is replaced with less humid air, allowing the product to dry. In general, the overall performance of the dryers is better in forced convection than in natural convection. A strong air flow rate leads to a more efficient overall transfer of warmth and hence, a reduction in the relative humidity, improving the drying process. Lower air flow rate causes poor drying performance [12]. In addition, forced convection with the appropriate design ensures that the generated air flow is nearly uniform on a flow cross-sectional width of the dryer.

Taking these factors into account, the most appropriate dryer is an active dryer with forced ventilation. We recommend to use axial fans as ventilation system, but this decision is up to the user and do not affect the design procedure. Fans can be powered by a photovoltaic solar panel and therefore do not require any non-solar energy nor extra operating costs.

### 1.3.2 Air heating mode

#### a) Direct sun dryers

The structure of direct sun dryers (Fig. 1.3) is simple. The product is generally isolated from the ambient air with transparent plastic cover. The sun shines directly on the product and increases the temperature inside the food storage. The transparent plastic cover creates a green house effect, which is also responsible for the increase of air temperature.

#### b) Indirect sun dryers

In indirect sun dryers (Fig. 1.4), the product is not directly in contact with the sunlight. The solar radiation is used to heat the air, which then flows through the product to be dried, usually thanks to some ventilation system. It is easier to reach high and controllable temperatures in indirect sun dryers if a fan is used to move the air through the solar collector. In this type of dryer, the product is also protected from ultraviolet light (UV). This can be an important feature for foods which lose nutritional value when exposed to direct sunlight.

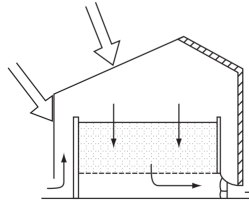


Figure 1.3: Example of an active direct sun dryer. Black arrows represent the air flow, white arrows represent the solar radiation flux [13]

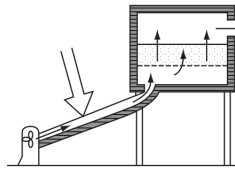


Figure 1.4: Example of an active indirect sun dryer [13]

Experiments have shown that indirect sun dryers are more efficient, but also more expensive compared to direct sun dryers [14]. In consequence, indirect solar dryer are more suitable for industrial or semi industrial applications, while direct solar dryer are more appropriate to a family-scale traditional drying. Therefore, we will not use an indirect sun dryer.

### c) Mixed mode dryers

Mixed mode dryers (Fig. 1.5) combine the characteristics of direct and indirect sun dryers. The air is pre-heated and the sun shines on the product and the pre-heated air. Experiments have shown that mixed mode dryers perform better than direct sun dryers. The mixed modes solar dryer is capable to dehydrate vegetables to a moisture content of below 10%. It also operates faster than the direct sun dryers [15].

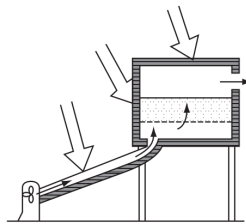


Figure 1.5: Example of an active mixed mode sun dryer [13]

### d) Hybrid mode dryer

The main disadvantage of solar drying systems in general is that they require adequate solar radiation. In hybrid mode dryers, the air is heated using solar energy in addition to another source of non-solar energy (i.e. fossil, fuel or biomass). Such technology gives the ability to operate without sun, which also allows better control of drying. In addition, fuel mode drying may be up to 40 times faster than solar drying [4].

Despite all the advantages of hybrid mode dryer, we do not use this technology because of its additional costs. Small-scale farmers may not be able to afford the electricity or other fuel for drying. Moreover, such dryers could create fuel dependence, which we prefer to avoid.

### 1.3.3 Box-type, cabinet and tunnel solar dryer

Box-type solar dryers (Fig. 1.6) consist of a drying chamber, a tray and a solar absorber combined into one unit. The air enters into the dryer thanks to air inlet holes, passes around the product while absorbing its moisture, and then leaves the dryer through the air outlet holes. Compared to the cabinet and the solar dryer described below, the box-type type dryer does not involve mix source of energy because the air is not heated before it reaches the product. As mentioned before, the drying process is more efficient when the air is pre-heated. Hence, our model does not consider this type of dryer.

Cabinet solar dryers (Fig. 1.7) are composed of a cabinet (large wooden or metal box) containing trays on which the product is located. The air is heated in a solar collector, then it passes through the stack of trays while drying the product. The heated air enters first in contact with the bottom tray, meaning this tray will dry first. The tray at the top of the cabinet is the last one to dry. This type of dryer is convenient because it requires less floor area to dry a certain amount of product compared to other dryers. The disadvantage of the cabinet solar dryer is that it tends to over-dry the products on the lower trays. Hence, it requires human intervention during the drying process to swap the trays. In developing countries, the floor area is usually not a constraint. Since we prefer to limit human intervention during the drying process, we do not use a cabinet solar dryer.

Tunnel solar dryers (Fig. 1.8) consist of a flat plate placed on a support above the ground and surrounded by glass or plastic sheets. The product is placed on a tray inside the dryer. The air enters through air inlet holes and is heated by direct sun radiation. Warmed air then flows around the product, absorbs its moisture and goes out through air vents or a chimney.

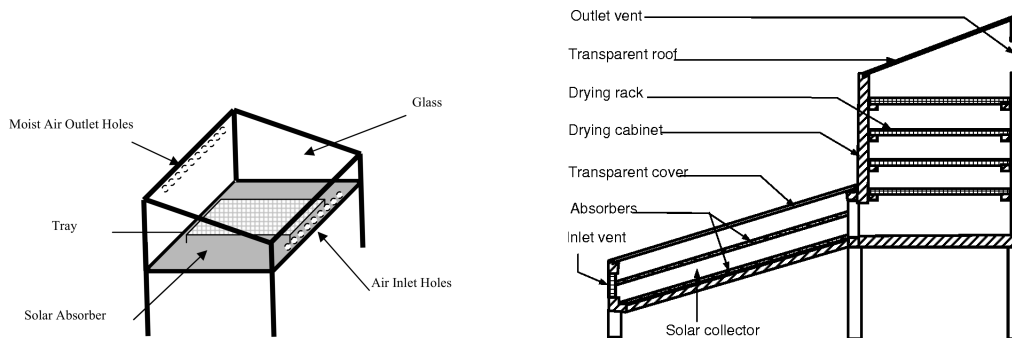


Figure 1.6: Schematic of a box-type solar dryer (direct) [16]

Figure 1.7: Sectional view of a cabinet solar dryer (mixed mode) [17]

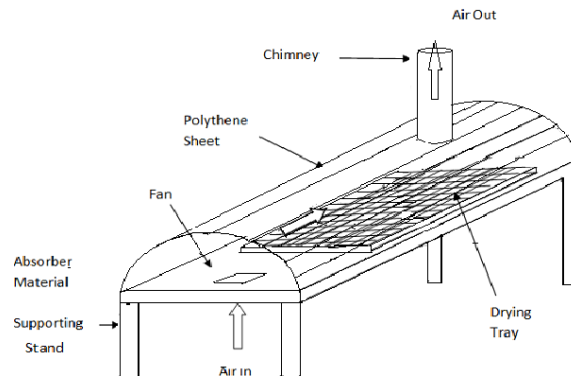


Figure 1.8: Schematic of a tunnel solar dryer [18]

### 1.3.4 Description of the dryer considered in this work

On the basis of the considerations above, we choose to develop a model and a software to design a tunnel solar dryer operating in mix mode with forced convection. Fig. 1.9 presents the overall structure of the dryer design.

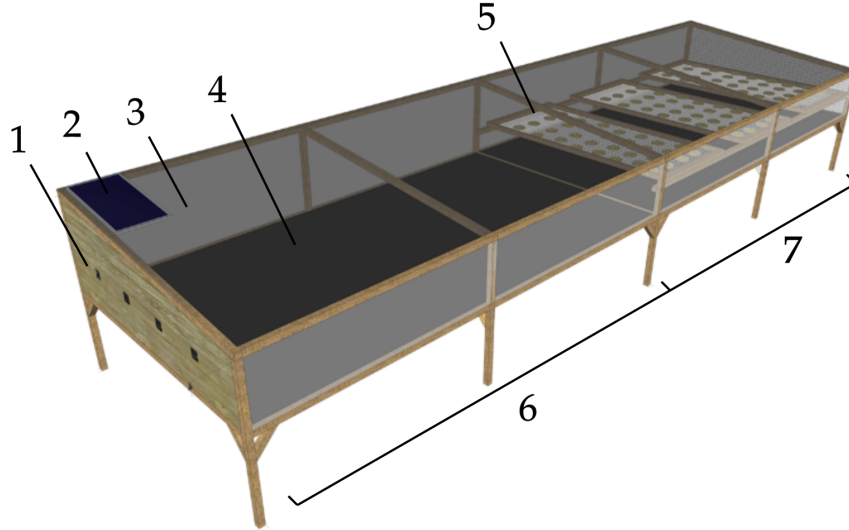


Figure 1.9: Schematic drawing of a ventilated tunnel solar dryer (adapted from [6]): (1) fans, (2) photovoltaic module, (3) transparent plastic sheet, (4) black matte floor, (5) tray with products to dry, (6) heating part, (7) drying part

Fans are powered by a photovoltaic module. An airflow is generated in the dryer. The dryer is composed of two parts.

The first part of the dryer is called the heating zone. In this zone, there are no products to dry. The air is at ambient temperature when it enters the heating zone. The air moves through the dryer and is heated thanks to the greenhouse effect produced by the combination of a black floor and a cover made of transparent plastic.

The second part of the dryer is called the drying zone. In this zone, the products to be dried are placed on trays. The products are in contact with the previously heated air and with direct solar radiations. In contact of the warmed air, part of the water contained inside the products is evaporated. The produced water vapor is transferred to the air. The air leaves the dryer through outlets located at the end of the drying zone.

A tunnel dryer is therefore a dryer combining a direct energy supply (solar radiation) and indirect (the air is heated in the heating zone).

We choose to narrow users possibilities by fixing the flow cross section of the dryer in size and in shape (see Section 1.3.4). As a consequence, the purpose of the model and of the software developed in this work is to determine the air ventilation rate and the lengths of the heating and drying zones in order to meet user requirements.



## Chapter 2

# Model and design procedure

### 2.1 Introduction

This chapter presents how to model and design a ventilated tunnel solar dryers. Section 2.2 presents the parameters that should be collected ahead of the design procedure. The underlying assumptions used to model the dryer and the design conditions are described in Section 2.3. In Section 2.4, we show how to calculate the ventilation system and the lengths of the heating and the drying zones of the dryer, based on the resolution of energy and mass balance equations and on the scope statement. Finally, Section 2.5 explains the numerical implementation of the design procedure.

### 2.2 Main parameters involved in the design procedure

The main parameters involved in the design procedure are divided in three categories: climatic data, product specifications and geometry of the dryer. Table B.1 presents the different parameters of each category. Some of these parameters are imposed by external conditions, others are fixed by us and the rest are based in the scope statement of the user. This section describes these parameters and their type, and gives an order of magnitude for some of them.

#### 2.2.1 Climatic data

Climatic data fully depend on the geographical position chosen for the construction of the dryer and on the period of the year. There are few constraints on the geographical position, except that the amount of sunshine must be relatively high and constant. Since the dryer developed is intended for developing countries, it is assumed that these constraints are fulfilled.

The climatic data are: the mean diurnal atmospheric infrared radiation flux  $I_{\text{atm}}$ , the mean diurnal direct and diffuse solar radiation flux  $S_{\text{atm}}$ , the mean ambient air relative humidity  $\text{RH}_{\text{amb}}$ , the mean diurnal ambient temperature  $T_{\text{amb}}$  and the sunrise  $t_{\text{rise}}$  and sunset time  $t_{\text{set}}$ .

The user should measure the values of the climatic data on the site of the drying. In the case the user do not have the possibility to do these measurements, many free online resources give the value of the data based on the geographical position [19][20][21].

#### 2.2.2 Product specifications

Product specifications are part of the scope statement defined by the user. For small-scale farmers communities, the mass of product to dry  $M_0$  is usually around 20 kg.

The drying temperature  $T_d$  and the drying time  $t_d$  are two important parameters. They depend on the type of product and the thickness of the slices to dry. The drying time is highly influenced by the slice thickness and the drying temperature. Appendix A presents the drying time of different fruits for several slice thicknesses and drying temperatures. For instance, going from a 4 mm to a 6 mm slice thickness increases the drying time by 69 %. Increasing the drying temperature of

Parameter	Description	Units
<i>Climatic data</i>		
$I_{\text{atm}}$	Mean diurnal atmospheric infrared radiation flux	W/m <sup>2</sup>
$RH_{\text{amb}}$	Mean diurnal ambient air relative humidity	%
$S_{\text{atm}}$	Mean diurnal direct and diffuse solar radiation flux	W/m <sup>2</sup>
$T_{\text{amb}}$	Mean diurnal ambient temperature	K
$t_{\text{rise}}$	Sunrise time	s
$t_{\text{set}}$	Sunset time	s
<i>Product specifications</i>		
$M_0$	Mass of product to dry	kg
$T_d$	Drying temperature	K
$t_d$	Drying time	s
$X_0$	Initial moisture content of product	kg water/kg dry product
$X_f$	Final moisture content of product	kg water/kg dry product
<i>Geometry of the dryer</i>		
$W_d$	Width of the dryer	m
$W_p$	Length of the cross section of the plastic cover transverse to the flow	m

Table 2.1: Data to collect before starting the design procedure

10 °C leads on average to a 11 % decrease in the drying time. To summarize, the four parameters (1) product type, (2) slice thickness, (3) drying temperature and (4) drying time are highly correlated. As a consequence, the user should take great care to introduce accurate value for  $t_d$  and  $T_d$ .

The value of the drying temperature  $T_d$  is crucial. The moisture absorption capacity of the air depends on its humidity and its temperature. Warm air can hold more moisture than cold air. Hence,  $T_d$  should be chosen as high as possible. However, too important temperatures destroy nutrients within the food itself and modify the color of the product. Typically, it is best to use drying temperature between 50 °C and 70 °C [22].

The drying model developed in this work is intended for one day drying. Hence, the value of  $t_d$  should respect the constraint:  $t_d \leq t_{\text{set}} - t_{\text{rise}}$ . Multi-day drying could be the subject of model improvements later.

The initial moisture content of the product  $X_0$  depends on the type, the variety and the maturation of the product. In order to determine the initial moisture content, the procedure described in [23] can be followed. It consists in a 30 minutes heating in a microwave oven under certain conditions. The final moisture content of the product  $X_f$  is chosen by the user in order to meet the expected quality of the product.

### 2.2.3 Geometry of the dryer

The geometry of the dryer is not determined by external constraints and the shape of the flow cross section is a priori arbitrary. However, we decide to impose a trapezoidal shape for the flow cross section of the dryer as shown in Fig. 2.1. The choice eases the design process for the user since he do not need to worry about the geometry of the dryer. In addition, a trapezoidal shape is easier to build compared to others shapes (e.g. a semi-circle).

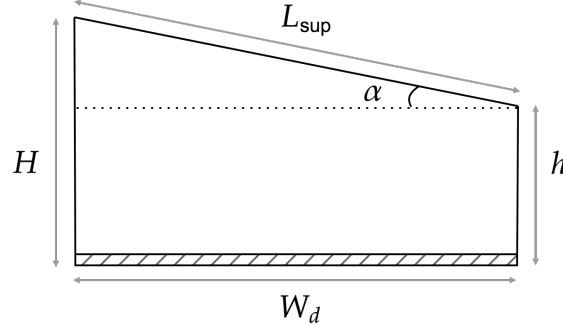


Figure 2.1: Schematic flow cross section of the dryer designed

Similarly to the shape, the dimensions of the width  $W_d$  and the heights  $H$  and  $h$  are arbitrary. We decide to fix the dimensions to  $W_d = 1.5$  m,  $h = 0.3$  m and  $H = 0.5$  m. It instantly sets the values of  $\alpha \approx 7.80^\circ$  and  $L_{\text{sup}} \approx 1.53$  m, using Eq. (2.1) and Eq. (2.2). These dimensions have been tested and validated by Talbot et al. in Uganda and are known to perform well. A higher value of the width makes complicates the manipulation of the trays. The values for the heights facilitate the insertion of the trays, and the value of the angle  $\alpha$  ensures a good drain of water in case of rain.

$$\alpha = \arctan\left(\frac{H - h}{W_d}\right) \quad (2.1)$$

$$L_{\text{sup}} = \sqrt{W_d^2 + (H + h)^2} \quad (2.2)$$

The aspect ratio of the flow cross section of the dryer  $R$  is defined as the ratio between the width of the dryer  $W_d$  and the length of the cross section of the plastic cover transverse to the flow  $W_p$ , with  $W_p = H + h + L_{\text{sup}}$

$$R = \frac{W_p}{W_d} \quad (2.3)$$

Using the dimensions defined, the value of the cross section of the plastic cover is  $W_p \approx 2.33$  m and the aspect ratio parameters is  $R \approx 1.55$ . The aspect ratio is involved in the modelling of the heat transfers taking place in the dryer (see Section 2.4.2).

## 2.3 Assumptions and design condition

### 2.3.1 Assumptions

The model developed in this work is an approximation of reality. Three main assumptions are made in order to simplify the model without degrading its results.

First, we assume that all climatic data are constant in time during the day, except for the diurnal direct and diffuse solar radiation  $S(t)$ . A sensitivity analysis from Talbot et al. has shown that  $S(t)$  is by far the most sensitive input of the procedure. As a result, we set the other climatic data  $T_{\text{amb}}$ ,  $I_{\text{atm}}$  and  $\text{RH}_{\text{amb}}$  equal to their average value over the day because they have much less

impact on the dimensions of the dryer than  $S(t)$ .

Second, we assume that the temperatures of the outer and inner surfaces of the plastic cover are equal. A conductive heat flux  $D$  takes place inside the thickness of the plastic layer. This flux is expressed as the product of a heat transfer coefficient and the temperature difference [24]:  $D = \lambda_p/e_p \Delta T_p$ , where  $\lambda_p$  the plastic thermal conductivity,  $e_p$  the thickness of the plastic layer and  $\Delta T_p$  the temperature difference between the outer and the inner surface of the plastic. The heat transfer coefficient within the plastic  $\lambda_p/e_p$  is several orders of magnitude larger compared to the other transfer coefficients of the system, but the heat passing through the plastic is of the same order of magnitude as all other heat transfers taking place inside the dryer. Therefore, the temperature difference is very small compared to other temperature differences of the system. This assumption eases the numerical resolution of the design procedure since two unknowns are combined into one, but it does not significantly impact the results of the design procedure.

Third, we assume that energy and mass transfers are at quasi-steady-state in the dryer. The characteristic times of the energy and mass transfers are a few seconds, while the time of the drying operation is a few hours. Considering the different order of magnitude, the quasi-steady state assumption is reasonable.

### 2.3.2 Design conditions

The design conditions should ensure that the drying process is efficient and homogeneous. Three conditions have to be fulfilled to obtain final product with a low and uniform moisture content.

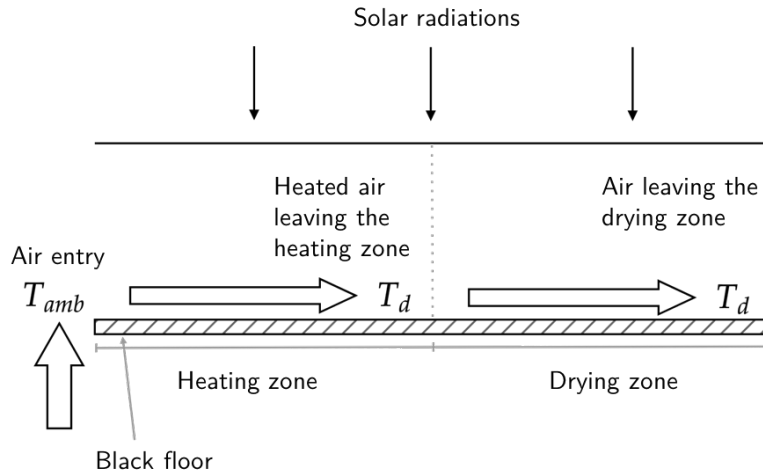


Figure 2.2: Air flow in the solar tunnel dryer. The design conditions impose that, on average, the air leaving the heating zone is at temperature  $T_d$  and that, on average, the air temperature at the end of the drying zone is  $T_d$  as well.

First, the relative humidity of the air inside the dryer should remain far below 100 %, namely far below saturation, to ensure homogeneous drying. Indeed, the humidity of the air has an influence on evaporation and thus on the drying efficiency as well. A relative humidity of 100 % means the air is completely saturated with vapor water and cannot absorb any more water. Low air humidity leads to higher evaporation rate. This condition guides the determination of the air flow rate of the ventilation system.

Second, the air temperature at the end of the heating part averaged during the drying time should be equal to the drying temperature  $T_d$ . This condition is used in the determination of the length of the heating part of the dryer.

Finally, the net energy captured in the drying part (energy brought by the sun radiations) should, on average, balance the energy needed for the evaporation of water in the products. To put it another way, the air temperature at the end of the drying part averaged during the drying time should also be equal to  $T_d$ , this ensuring homogeneous drying. This condition is used in the determination of the length of the drying part of the dryer.

## 2.4 Design of the dryer

The design procedure of the dryer is divided in two steps. The first step is to design the ventilation system to ensure that the humidity of the air inside the dryer remains far from saturation. The second step is to determine the lengths of the heating and the drying parts. In order to do so, we solve energy and mass balance equations on the basis of the different energy transfers taking place inside the dryer.

### 2.4.1 Design of the ventilation system

The humidity of air saturated with water at air temperature  $T$  is the maximum amount of vapor water the air can contain at a certain temperature. This humidity  $Y_{\text{sat}}(T)$ , expressed in kg water/kg dry air, is calculated as follow:

$$Y_{\text{sat}}(T) = \frac{\widehat{M}_w \frac{P_{\text{sat}}(T)}{P_{\text{atm}}}}{\widehat{M}_a \left(1 - \frac{P_{\text{sat}}(T)}{P_{\text{atm}}}\right)} \quad (2.4)$$

where  $\widehat{M}_a$  and  $\widehat{M}_w$  are respectively the molar mass of air and water,  $P_{\text{atm}}$  is the atmospheric pressure and  $P_{\text{sat}}(T)$  is the saturation pressure of water at the temperature  $T$  (tabulated for example in [25]).

The mean diurnal ambient humidity  $Y_{\text{amb}}$  is then calculated with:

$$Y_{\text{amb}} = \text{RH}_{\text{amb}} Y_{\text{sat}}(T_{\text{amb}}) \quad (2.5)$$

The minimal air flow rate  $Q_{\text{min}}$ , expressed in kg humid air/s, is defined as the air flow rate that would lead to an air saturated with water and at temperature  $T_d$  at the exit of the dryer. It can be computed by expressing a mass balance equation.

The initial mass of fresh product  $M_0$  is the sum of the initial mass of water in the product  $M_{w,0}$  and the mass of dry product  $M_{dp}$ :  $M_0 = M_{w,0} + M_{dp}$ . The initial humidity  $X_0$  is the ratio  $M_{w,0}/M_{dp}$ . These two relations are combined to express the mass of dry product.

$$M_{dp} = \frac{M_0}{1 + X_0} \quad (2.6)$$

The final mass of water in the product  $M_{w,f}$  is the product of the mass of dry product and the final humidity  $X_f$ ,  $M_{w,f} = M_{dp} X_f$ . Hence, the mass of water to evaporate  $M_{w,\text{evaporate}}$  is given by:

$$M_{w,\text{evaporate}} = M_{w,0} - M_{w,f} = M_{dp}(X_0 - X_f) = \frac{M_0}{1 + X_0}(X_0 - X_f) \quad (2.7)$$

The minimal air flow rate  $Q_{\text{min}}$ , expressed in kg humid air/s, is computed using the following mass balance equation:

$$Q_{\text{min}} \frac{Y_{\text{sat}}(T_d) - Y_{\text{amb},m}}{1 + Y_{\text{amb},m}} = \frac{M_0}{1 + X_0} (X_0 - X_f) \frac{1}{t_d} \quad (2.8)$$

Eq. (2.8) represents that the mass of water absorbed by the air per second is equal to the mass of water to evaporate averaged on the drying time.

Using  $Q_{\text{min}}$  as an air flow rate leads to a relative humidity of 100% at the exit of the dryer. As stated in Section 2.3.2, lower relative humidity allows faster drying, but also more homogeneous

drying. Hence,  $Q_{\min}$  is multiplied by a coefficient  $F$  to ensure that the relative humidity of the air in the dryer remains far below 100%.

$$Q = Q_{\min} F \quad (2.9)$$

Typically,  $F$  has a range between 10 and 15 [6]. In our model, we fix the coefficient  $F = 10$ , which has been demonstrated to be largely enough to keep low humidity in the dryer.

To achieve the required airflow, the user can use axial fans powered by a photovoltaic solar panel. A large fan in the middle of the entrance does not provide uniform ventilation, therefore we strongly advice the user to use smaller multiple fans (see Section 3.5.2).

### 2.4.2 Design of the heating and the drying parts

The next step of the design is to find out the minimum required lengths of the heating and drying parts. These lengths are calculated by solving energy balance equations. First, we describe the heat transfers taking place into the dryer. Then, we use the conservation of energy on three different systems to write energy balance equations. Finally, we impose the design condition explained in Section 2.3.2 to determine the lengths of the heating and drying parts.

The energy fluxes taking place inside the dryer are represented in a transversal cut in Fig. 2.3 for the heating and drying zones.  $T_{\text{amb}}$ ,  $T_p$ ,  $T_{\text{air}}$  and  $T_{\text{fl}}$  are respectively the temperatures of the ambient air outside the dryer, of the plastic cover, of the air inside the dryer and of the floor. These last three depend on the time of the day ( $t$ ) and on the longitudinal position inside the dryer ( $z$ ).

The black floor capture a fraction  $k$  of the direct and diffuse solar radiation flux ( $S$ ) and the plastic cover captures the atmospheric infrared radiation flux ( $I_{\text{atm}}$ ). The black floor heats and a greenhouse effect takes place inside the dryer. There is a net infrared energy flux exchange between the black floor and the plastic cover ( $I_{fl-p}$ ). An infrared radiation flux is also emitted by the plastic cover towards the atmosphere ( $I_p$ ). Convective heat transfers take place between the plastic and the ambient air ( $C_o$ ), between the plastic cover and the air inside the dryer ( $C_p$ ), and between the black floor and the air inside the dryer ( $C_{fl}$ ). These transfers are defined as positive when heat is transferred to the air. In the drying zone, energy is consumed by the evaporation of the water ( $EV$ ). All these energy fluxes are expressed in W per  $\text{m}^2$ .

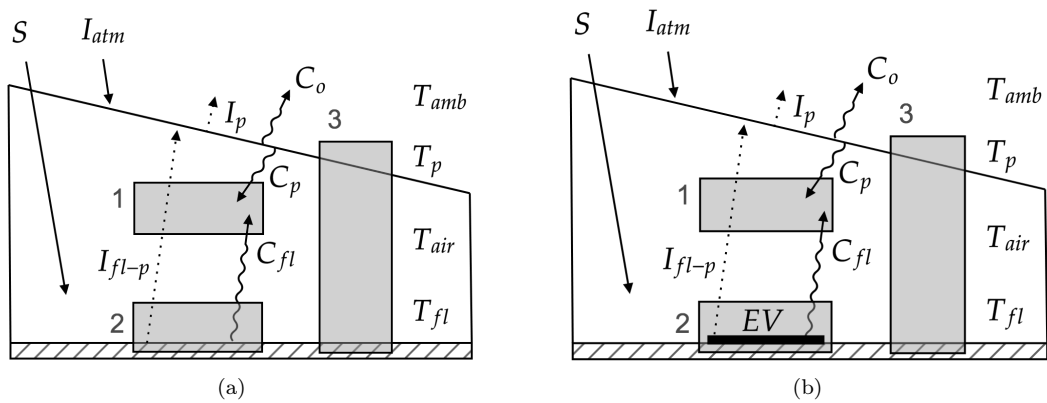


Figure 2.3: Energy fluxes (in  $\text{W}/\text{m}^2$ ) represented in a transversal cut of the (a) heating zone (b) drying zone. The 3 gray rectangles delimit the zones selected to express the energy balance equations

We write energy balance equations for the three rectangles in Fig. 2.3, where rectangle 1 is the air inside the dryer, rectangle 2 is the bottom of the dryer, and rectangle 3 is the entire flow cross section. The energy balance equations are Eq. (2.10), (2.11) and (2.13) for the heating zone, and Eq. (2.10), (2.12) and (2.13) for the drying zone.

$$\begin{cases} P = C_p + C_{fl} & (2.10) \\ S k = I_{fl-p} + C_{fl} & (2.11) \\ S k = I_{fl-p} + C_{fl} + EV & (2.12) \\ S + I_{atm} = C_o + I_p & (2.13) \end{cases}$$

$P$  is the the energy flux transferred to the air inside the dryer. This energy flux is used to heat the air in the heating zone, and to evaporate the water from the product in the drying zone.

Eq. (2.10) expresses the energy balance of the air at a given position inside the dryer. The energy flux transferred to the air is equal to the convective heat fluxes coming from the floor and from the plastic cover. Eq. (2.11) expresses the energy balance at the floor in the heating part. The fraction  $k$  of the direct and diffuse solar radiation flux captured by the floor is balanced by the net infrared flux exchanged with the plastic cover and by the convective flux with the air inside the dryer. Eq. (2.12) expresses the same energy balance but with an additional term accounting the energy loss due to evaporation. At last, Eq. (2.13) expresses a global energy balance for the system. The direct and diffuse solar radiation flux and the atmospheric infrared radiation are balanced by the energy losses due to infrared emission and to convection with the ambient air.

As mentioned, only a fraction  $k$  of the direct and diffuse solar radiation flux is captured by the black flat floor. Therefore, a reduction factor  $k$  is introduced to take into consideration that . Its value depends on the kind of plastic and on the wood structure used. It is usually around 0.85.

In the following subsections, we describe one by one how the different fluxes are expressed.

#### a) Direct and diffuse solar radiation flux

A realistic model of the direct and diffuse solar radiation flux  $S(t)$  is a sinusoidal model. The value of  $S(t)$  during the day can be expressed using the mean diurnal direct and diffuse solar radiation flux  $S_{atm}$ :

$$S(t) = \frac{\pi}{2} S_{atm} \sin \left( \pi \frac{t - t_{rise}}{t_{set} - t_{rise}} \right) \quad (2.14)$$

The flux is zero at sunrise and sunset time:  $S(t_{rise}) = S(t_{set}) = 0$ . The flux is maximal when  $t = (t_{rise} + t_{set})/2$ . The factor  $\pi/2$  ensures that the average flux during the day is  $S_{atm}$ . We define  $t_0$  as the drying starting time:

$$t_0 = \frac{t_{rise} + t_{set}}{2} - \frac{t_d}{2} \quad (2.15)$$

Eq. (2.15) ensures that the drying is done during the brightest hours of the day.

#### b) Convective heat flux

A convective heat transfer  $C$  is an energy transfer between a surface and a fluid moving over the surface. This type of exchange follows the Newton's law (Chapter 6 in [26]):

$$C = h\Delta T \quad (2.16)$$

where  $h$  is the convective heat transfer coefficient and  $\Delta T$  is the difference of temperature between the surface and its environment. The determination of the convective heat transfer coefficient  $h$  depends on the characteristics of the fluid but also on the flow conditions and the geometry considered. The convective heat transfer coefficient is evaluated empirically using dimensionless grouping of parameters relevant to the flow dynamics. These dimensionless groups have physical interpretations related to conditions in the flow.

The motion of the flow is caused by two phenomena that coexist: the motion is simultaneously caused by a difference of temperature resulting in a difference of density, phenomenon called natural convection, and by a mechanical mean, phenomenon called forced convection. Talbot et al. have calculated the values of the free convection and the forced convection heat transfer

coefficients. It appears that the forced convection heat transfer coefficient is negligible compared to the free convection one, due to the low values of the air velocity and to the high difference of temperature between the media exchanging energy. In consequence, we assume that the convective heat transfer inside the dryer is dominated by natural convection. Therefore, the convective heat transfer coefficient is evaluated with the empirical correlations (Chapter 10 in [27]):

$$\text{Nu} = hL_c/\lambda_a = 0.4\text{Ra}^{0.25} \quad (2.17)$$

where  $\text{Nu}$  is the Nusselt number,  $L_c$  is the hydraulic diameter of the flow cross section of the dryer,  $\lambda_a$  is the air thermal conductivity and  $\text{Ra}$  is the Rayleigh number. The Nusselt number is the ratio of convection to pure conduction heat transfer. The hydraulic diameter  $L_c$  is defined as the ratio between 4 times the area  $A$  and the perimeter  $P$ :

$$L_c = \frac{4A}{P} = \frac{\frac{W_d}{2}(H+h)}{W_d + H + h + L_{\text{sup}}} \quad (2.18)$$

All parameter involved in Eq. (2.18) are fixed in Section 1.3.4. Hence, the hydraulic diameter is  $L_c \approx 0.63$  m.

The Rayleigh number defined is the product of the Prandtl and the Grashof numbers (Chapter 9 in [26]):

$$\text{Ra} = \text{Pr Gr} = \frac{\nu_a \rho_a C_a}{\lambda_a} \frac{\beta_a g L_c^3 \Delta T}{\nu_a^2} \quad (2.19)$$

where  $\nu_a$  is the kinematic viscosity of the air,  $\rho_a$  is the air density,  $C_a$  is the air heat capacity,  $\beta_a$  is the thermal expansion coefficient of the air and  $g$  is the standard gravity. The fluid properties are evaluated at the mean temperature between the fluid and the surface. The Prandtl number depends only on fluid properties. The Grashof number characterizes natural convection and is a measure of the ratio of the buoyancy forces to the viscous forces in the fluid.

### c) Infrared radiation flux

All objects are emitting infrared radiations  $I$ . The emissivity of a body characterizes the efficiency in which the body emits thermal energy. A perfect emitter is called a black body and its emissivity is 1. Usually, the emissivity of plastic materials is larger than 0.9 and the emissivity of a black surface larger than 0.95 [24]. Hence, the plastic cover and the black floor can reasonably be considered as black bodies. Thus, their infrared radiation flux follows the Stefan-Boltzmann's law:

$$I = \sigma T^4 \quad (2.20)$$

where  $\sigma$  is the Stefan-Boltzmann's constant and  $T$  the temperature of the surface.

### d) Energy consumption due to evaporation

Water is extracted from the products by evaporation, a state change from liquid to vapor. Talbot et al. assume that the evaporation rate is constant over the drying time, but as mentioned previously, it is inaccurate. Consequently, in our model, we propose to express the drying rate  $J(t, T)$ , expressed in kg of water evaporated per second and per kg of dry product, as an exponentially decreasing function of time and an exponentially increasing function of temperature as follows:

$$J(t, T) = \alpha \underbrace{\exp\left(-4 \frac{(t-t_0)}{t_d}\right)}_{(1)} \underbrace{\exp\left(-\frac{E_a}{R_g} \left(\frac{1}{T} - \frac{1}{T_d}\right)\right)}_{(2)} \quad (2.21)$$

where  $\alpha$  is a drying coefficient,  $t_0$  is the drying starting time,  $E_a$  is the activation energy and  $R_g$  is the molar gas constant. The expression of  $J$  is the product of two term. The first term models the time dependency of the drying rate. It has been shown that modeling the time dependency with a decreasing exponential function is suitable for many products [8]. The drying rate should tend towards zero when the drying time  $t_d$  is reached. This justifies the introduction of the



factor 4 inside the exponential. Indeed, replacing  $t = t_0 + t_d$  gives a value of  $\exp(-4) \approx 0.02$  for term (1), which is close to zero as expected. The second term accounts for the temperature dependency of the drying rate. This dependency is modeled with an Arrhenius law. Such a model can well explain the experimentally observed rate of drying, for many products [28][29]. Based on laboratory experiments done previously by another student, we fix the activation energy to  $E_a = 10,000$  J/mol. The coefficient  $\alpha$  is chosen such as the equality below is satisfied.

$$\frac{1}{t_d} \int_{t_0}^{t_0+t_d} J(t - t_0, T = T_d) dt = \frac{X_0 - X_f}{t_d} \quad (2.22)$$

Eq. (2.22) expresses that the mean value of the drying rate function  $J$  over the total drying time  $t_d$  at the drying temperature  $T_d$  is equal to the averaged quantity of water to evaporate per kg of dry product and per second. Solving the definite integral on the left side of the equation and rearranging the terms gives the expression for the drying coefficient  $\alpha$ :

$$\alpha = \frac{4(X_0 - X_f)}{t_d (1 - e^{-4})} \approx \frac{4(X_0 - X_f)}{t_d} \quad (2.23)$$

Finally, the energy consumed by the evaporation of water  $EV$ , expressed in W/m<sup>2</sup>, is equal to:

$$EV(t) = \frac{M_S}{1 + X_0} L_w J(t, T) \quad (2.24)$$

where  $M_S$  is the mass of fresh products placed per unit floor area in the drying part, expressed in kg/m<sup>2</sup>, and  $L_w$  is the mass latent heat of vaporization, expressed in J/kg. The ratio  $M_S/(1 + X_0)$  represents the mass of dry product placed per unit floor area.

#### e) Energy balance equations

Now we have defined all the energy transfers taking place inside the dryer, we replace the fluxes in the energy balance equations Eq. (2.10)–(2.13) by their value:

$$\begin{cases} P(t, z) = h_{fl} (T_{fl}(t, z) - T_{air}(t, z)) + Rh_p(T_p(t, z) - T_{air}(t, z)) \end{cases} \quad (2.25)$$

$$\begin{cases} S(t)k = \sigma (T_{fl}^4(t, z) - T_p^4(t, z)) + h_{fl} (T_{fl}(t, z) - T_{air}(t, z)) \end{cases} \quad (2.26)$$

$$\begin{cases} S(t)k = \sigma (T_{fl}^4(t, z) - T_p^4(t, z)) + h_{fl} (T_{fl}(t, z) - T_{air}(t, z)) + \frac{M_S}{1 + X_0} L_w J(t, T) \end{cases} \quad (2.27)$$

$$\begin{cases} S(t) + I_{atm} = h^* (T_p(t, z) - T_{amb}) + \sigma T_p^4(t, z) \end{cases} \quad (2.28)$$

$$\begin{cases} C_a Q \frac{\partial T_{air}(t, z)}{\partial z} = P(t, z) W_d \end{cases} \quad (2.29)$$

Eq. (2.29) expresses an energy balance for the air inside the dryer, with  $C_a$  the air heat capacity expressed in J/kg/K. The energy captured by the sections of surface  $W_d \delta z$  is given by  $P W_d \delta z$ , and this power is only used to heat the air flow rate  $Q$  which passes through the dryer. This forms a system of 4 equations with 4 unknowns for the heating and the drying zones. The unknowns are  $P$ ,  $T_p$ ,  $T_{fl}$  and  $T_{air}$ .

#### f) Lengths of the heating and drying zones

The length of the heating section is calculated using the design conditions mentioned in Section 2.3.2 in addition to boundary conditions. At any time during the drying, air at the entry of the dryer is at ambient temperature:  $T_{air}(z = 0, t) = T_{amb}$ . Therefore, Eq. (2.25), (2.26) and (2.28) form a system of three equations with three unknowns ( $P$ ,  $T_{fl}$ ,  $T_p$ ). We discretize Eq. (2.29) and rearrange the terms, which gives:

$$\Delta T_{air} = \frac{P(z, t) W_d}{Q C_a} \Delta z \quad (2.30)$$

Since  $P(z, t)$  has been calculated in  $z = 0$ , we deduce the air temperature increase  $\Delta T_{air}$  over a small slice  $\Delta z$  with the relation above. The same reasoning is done on the next slice with this time

the air temperature  $T_{\text{air}}(z + \Delta z, t) = T_{\text{air}}(z, t) + \Delta T_{\text{air}}$ , and so on. The length of the heating zone  $L_H$  is determined by solving the the design condition:

$$\frac{1}{t_d} \int_{t_0}^{t_0+t_d} T_{\text{air}}(t, L_H) dt = T_d \quad (2.31)$$

This equation expresses that the air temperature at the end of the heating part ( $z = L_H$ ) averaged during the drying time should be equal to the drying temperature  $T_d$ .

The determination of the length of the drying zone is done using the last design condition explained in Section 2.3.2: the net energy captured in the drying part  $P$  should, on average, balance the energy needed for the evaporation of water in the products.

$$P(t, z = L_H) \stackrel{\text{on average}}{=} \frac{M_S}{1 + X_0} \mathcal{L}_w J(t, T_{\text{air}}(t, z = L_H)) \quad (2.32)$$

The only unknown from this equation is the mass of product per unit floor area  $M_S$ . Its value is found by rearranging the terms and solving the following integral:

$$M_S = \frac{1 + X_0}{\mathcal{L}_w} \frac{\int_{t_0}^{t_0+t_d} P(t, z = L_H) dt}{\int_{t_0}^{t_0+t_d} J(t, T_{\text{air}}(t, z = L_H)) dt} \quad (2.33)$$

The mass of product per unit area  $M_S$  is the ratio between the total mass of fresh product and the total floor area of drying zone. Hence, the length of the drying zone  $L_D$  is determined with the following equation:

$$M_S = \frac{M_0}{L_D W_d} \quad (2.34)$$

It is important to note that the value of  $M_S$  should not exceed  $M_{S,\text{max}}$ , the maximum mass of fresh products possible to place per  $\text{m}^2$  of floor area in the drying part. The value of  $M_{S,\text{max}}$  depends on the thickness of the slices  $e$ , the density of the product  $\rho_{\text{product}}$  and the arrangement in which the products are disposed. Fig. 2.4 is a schematic of a product slice and Fig. 2.5 represents one way to dispose the products on the floor. The arrangement represented is not the most compact one, but this gives already a good approximation of  $M_{S,\text{max}}$ .

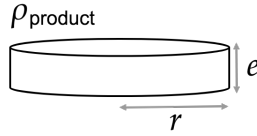


Figure 2.4: Schematic of a product slice

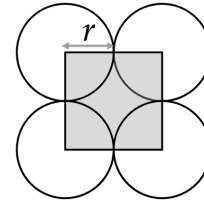


Figure 2.5: Schematic top view of the products disposed on the floor

The mass of a product slice is given by  $\pi r^2 e \rho_{\text{product}}$ . The maximum mass of fresh product per floor area is the ratio between the mass of product inside the gray square of Fig. 2.5 and the area of the same square :

$$M_{S,\text{max}} = \frac{\rho_{\text{product}} \pi r^2 e}{4 r^2} = \frac{\rho_{\text{product}} \pi e}{4} \quad (2.35)$$

In the case  $M_S > M_{S,\text{max}}$ , it means that the scope statement is not compatible with the design conditions and that it should be revised ( $M_0$  should be lowered).

## 2.5 Numerical resolution

The resolution of the design procedure is done numerically with Python. This section describes the main steps of the algorithm developed. The algorithm first calculates the minimal air flow rate required, then it calculates the length of the heating section and finally it calculates the length of the drying section.

The algorithm receives the inputs mentioned in Section 2.2. The determination of the air flow rate is straightforward since all equations of the design of the ventilation system are first order equations (see Section 2.4.1).

The next step is to calculate the length of the heating section. We fix the maximum length of the heating zone  $L_{H,\max}$  to 10 meters to ensure reasonable dimensions for the dryer. The non-linear system of equations (2.25)–(2.29) is solved (using `fsolve` function from `scipy.optimize` library) for  $z = 0$  to  $z = L_{H,\max}$  at time  $t = t_0$ . The same procedure is repeated for  $t = t_0 + \Delta t$  until  $t = t_0 + t_d$  is reached. At this point, all values of  $T_{\text{air}}, T_p, T_{fl}$  and  $P$  are known for every  $z \in [0, L_{H,\max}]$  and  $t \in [t_0, t_0 + t_d]$ . All values of  $P(t, z)$  and  $T_{\text{air}}(t, z)$  are kept in memory.

Then, the algorithm evaluates the mean value of the air temperature  $T_{\text{air}}$  at the end of the heating section  $z = L_{H,\max}$ . The target value of the mean air temperature is the drying temperature  $T_d$  with a certain tolerance  $\epsilon$ . We approximate the integral of Eq. (2.31) with a Darboux sum. Three scenarios can occur.

- The mean value of  $T_{\text{air}}(t, z = L_{H,\max}) = T_d \pm \epsilon$ . In that case, the heating length is  $L_H = L_{H,\max}$  since it fulfills the design condition.
- The mean value of  $T_{\text{air}}(t, z = L_{H,\max}) < T_d - \epsilon$ . It means that the heating length should be higher than  $L_{H,\max}$ . The algorithm will stop there and inform the user that the scope statement should be revised because it leads to a very long value for the heating length.
- The mean value of  $T_{\text{air}}(t, z = L_{H,\max}) > T_d + \epsilon$ . It means that the heating length should be lower than  $L_{H,\max}$ . A dichotomic search is done on the value of  $L_H$ . The algorithm has already calculated the values of  $T_{\text{air}}(t, z = L_{H,\max}/2)$  from the previous step. It evaluate the mean value of the air temperature at the end of the heating section and it continues the dichotomic search until a value of  $L_H$  fulfilling the design condition is found.

In the current version of the algorithm, the value of the tolerance is  $\epsilon = 2.5^\circ\text{C}$  and the steps are  $\Delta z = 0.1$  m and  $\Delta t = 30$  minutes.

Once the heating length has been determined, the next step is to calculate the drying length. The values of  $P(t, z = L_H)$  and  $T_{\text{air}}(t, z = L_H)$  have already been calculated. The mean value of the mass of fresh product per floor area  $M_S$  is calculated with Eq. (2.33), where the integral is approximated with a Darboux sum. Finally, the value of  $L_D$  is determined by dividing the mass of fresh product per floor area by the width  $W_d$  of the dryer (Eq. (2.34)). In the current version of the algorithm, it is not checked whether the value of  $M_S$  is coherent or not (i.e.  $M_S \leq M_{S,\max}$ ), but this could be the subject of model improvements later.

Finding the optimal heating length is the most time consuming step of the algorithm. Indeed, the program has to solve  $\frac{L_{H,\max}}{\Delta z} \times \frac{t_d}{\Delta t}$  non-linear systems. In the conditions mentioned above, the algorithm has to solve 200  $t_d$  non-linear systems. For example, if the drying time is  $t_d = 6.5\text{h}$ , it represents 1300 systems and the resolution takes around 11 minutes with an Intel Core i5 processor with a 2.4 GHz clock and 4 GB of RAM.

## 2.6 Results of the design procedure for two situations

The purpose of this section is to apply our design procedure on two concrete cases, in order to illustrate the design procedure. We take the example of the drying of mango slices in Cambodia and of the drying of pineapple slices in Uganda. These two cases have been previously studied by Talbot et al. [6]. The input parameters of the model (scope statement and climatic data) associated to each situation are given in Table 2.2. The results of the design procedure are detailed below.

Symbol	Value		Units
<i>Climatic data</i>			
Site	Banlung, Cambodia	Jinja, Uganda	–
Period of the year	February–March	December–March	–
$I_{\text{atm}}$	377	322	W/m <sup>2</sup>
$RH_{\text{amb}}$	70	35	%
$S_{\text{atm}}$	463	613	W/m <sup>2</sup>
$T_{\text{amb}}$	30	28	°C
$t_{\text{rise}}$	7	6	h
$t_{\text{set}}$	19	18	h
<i>Products data</i>			
Product	Slices of mangoes	Slices of pineapples	–
$M_0$	10	25	kg
$T_d$	60–65	70–75	°C
$t_d$	6.5	8	h
$X_0$	7	6	kg water/kg dry product
$X_f$	0.1	0.3	kg water/kg dry product
$M_{S,\text{max}}$	2.4	6.0	kg product/m <sup>2</sup>

Table 2.2: Scope statement and data collected of the dryers built in Cambodia and in Uganda. Climatic data come from online resources and measurements on the field [6]

Symbol	Cambodia	Uganda	Units
$Q$	0.0247	0.0233	kg humid air/s
$L_H$	2.2	2.3	m
$M_S$	1.70	2.55	kg product/m <sup>2</sup>
$L_D$	3.92	6.55	m

Table 2.3: Results of the design procedure

Table 2.3 presents the determined values of  $Q$ ,  $L_H$ ,  $M_S$  and  $L_D$  when the design procedure is applied using the data presented in Table 2.2. The orders of magnitude of the air flow rate and of the lengths of the dryer are coherent. However, no deduction can be made regarding the validity of the model proposed in this work. In order to do so, results obtained theoretically should be verified through several drying experiments on the field. Field drying experiments could be the subject of further research (see Section 4.2.1).

### 2.6.1 Cambodia

The design procedure is applied to the Cambodia scope statement. The air flow rate is 0.0247 kg air/s, or 84.4 m<sup>3</sup>/h (with air density evaluated at  $T = 62^\circ\text{C}$ ). The determined length for the heating section is  $L_H = 2.2$  m. The temperature of the air at the end of the heating section  $T_{\text{air}}(t, z = L_H)$  is shown in Fig. 2.6. The mean temperature over the drying time is  $62.8^\circ\text{C}$ , which fulfill the scope statement ( $60\text{--}65^\circ\text{C}$ ). The maximum temperature obtained is  $67.5^\circ\text{C}$ , so there is no risk to change the color nor destroy the nutriment within the product. Fig. 2.7 shows the energy flux transferred to the air inside the dryer at the end of the heating section  $P(t, z = L_H)$ .

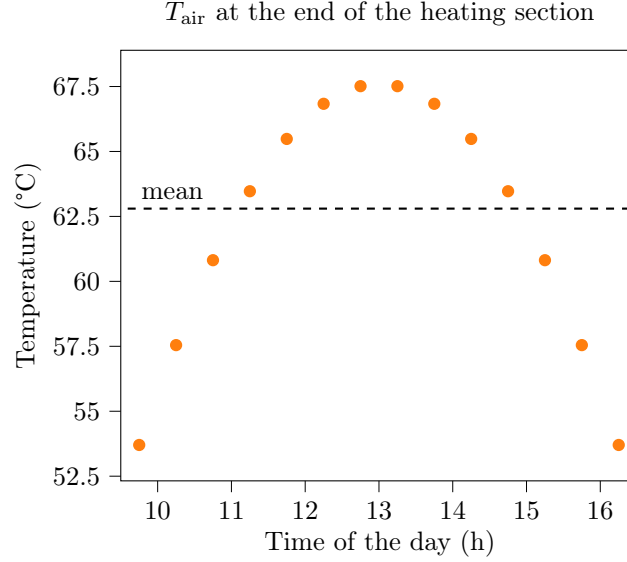


Figure 2.6: Temperature of the air  $T_{\text{air}}$  at the end of the heating section for  $L_H = 2.2$  m with the scope statement of Cambodia. The starting drying time is 09:45 am and total drying time is 6.5h. The mean temperature of the air at the end of the heating section is  $62.8^\circ\text{C}$

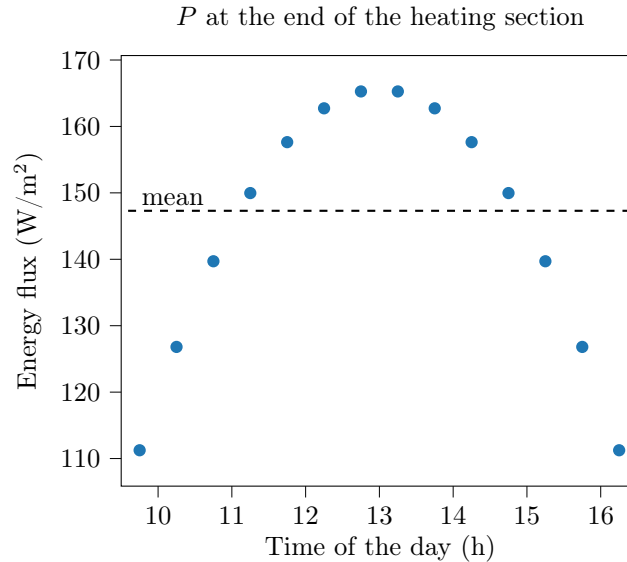


Figure 2.7: Energy flux transferred to the air inside the dryer  $P$  at the end of the heating section for  $L_H = 2.2$  m with the scope statement of Cambodia. The mean value of  $P$  is  $147.3 \text{ W/m}^2$

The length of the drying section is  $L_D = 3.92$  m, which gives a total length of 6.12 m for the entire dryer. The mass of product per unit floor area  $M_S$  is  $1.7 \text{ kg/m}^2$ , which is below the maximum mass of fresh products possible to place per m<sup>2</sup> of floor area. Fig. 2.8 shows the drying rate at the end

of the heating section  $J(t, z = L_H)$ . As stated in Section 2.4.2, the drying rate is an exponentially decreasing function of time. When the drying time is reached, the value of  $J(t = t_d, z = L_H) \approx 0$ .

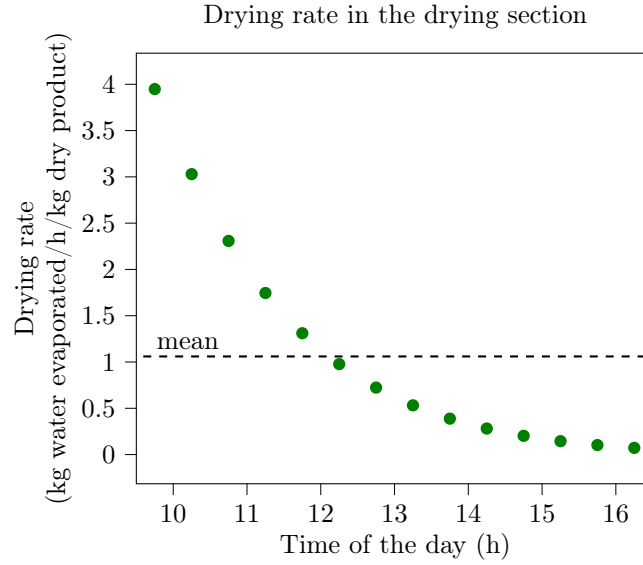


Figure 2.8: Drying rate  $J$  with the scope statement of Cambodia. The mean drying rate is 1.06 kg of water evaporated per hour and per kg of dry product

### 2.6.2 Uganda

The design procedure is applied to the Cambodia scope statement. The air flow rate is 0.0233 kg air/s, or 81.5 m<sup>3</sup>/h (with air density evaluated at  $T = 70^\circ\text{C}$ ) The determined length for the heating section is  $L_H = 2.3$  m. The temperature of the air at the end of the heating section  $T_{\text{air}}(t, z = L_H)$  is shown in Fig. 2.9. The mean temperature over the drying time is 70.4  $^\circ\text{C}$ , which fulfill the scope statement (70–75  $^\circ\text{C}$ ), and the maximum temperature obtained is 80.0  $^\circ\text{C}$ . In this case, it should be checked that this temperature does not damage the pineapples.

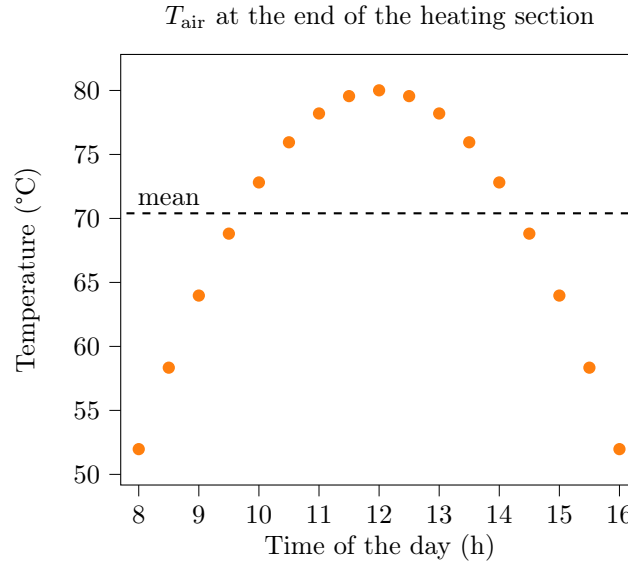


Figure 2.9: Temperature of the air  $T_{\text{air}}$  at the end of the heating section for  $L_H = 2.3$  m with the scope statement of Uganda. The starting drying time is 08:00 am and total drying time is 8h. The mean temperature of the air at the end of the heating section is 70.4  $^\circ\text{C}$

Fig. 2.10 and Fig. 2.11 respectively show the energy flux transferred to the air inside the dryer at the end of the heating section and the drying rate in the drying section. The length of the drying section is  $L_D = 6.55$  m, which gives a total length of 8.85 m for the entire dryer. The mass of product per unit floor area  $M_S$  is  $2.54 \text{ kg/m}^2$ , which is below  $M_{S,\max}$ .

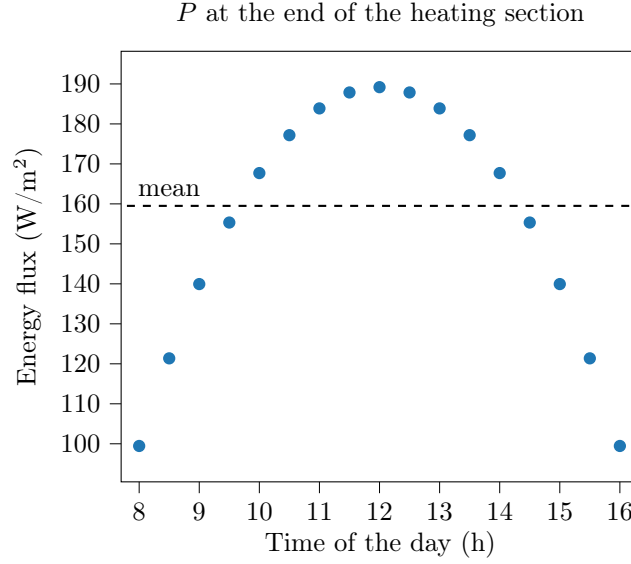


Figure 2.10: Energy flux transferred to the air inside the dryer  $P$  at the end of the heating section for  $L_H = 2.3$  m with the scope statement of Uganda. The mean value is  $159.6 \text{ W/m}^2$

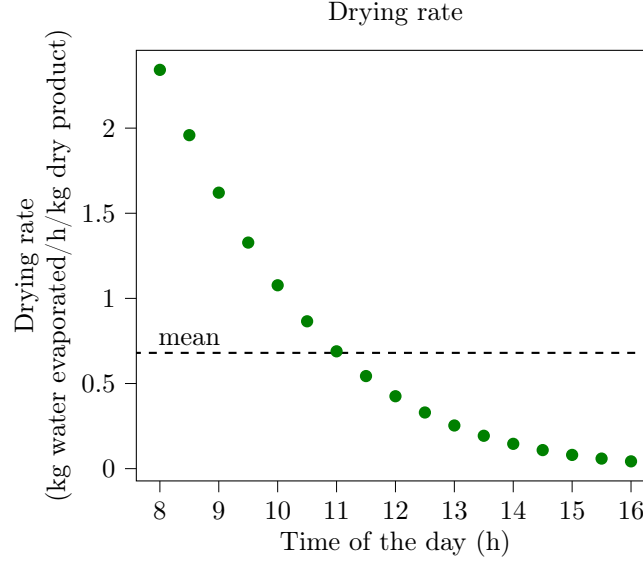


Figure 2.11: Drying rate  $J$  with the scope statement of Uganda. The mean drying rate is  $0.68 \text{ kg}$  of water evaporated per hour and per  $\text{kg}$  of dry product

## Chapter 3

# Open access software

### 3.1 Introduction

This chapter presents the open-source software we have developed in the context of this work. The software provides an interface for users to interact with, and exploit the model described in the previous chapter without the need to understand its implementation. The purpose of the software is to help a user to determine easily the optimal dimensions of a simple tunnel solar dryer that meets user expectations. The principle is simple: the user enters the specifications, and the program returns the air flow required and the dimensions of the dryer. All the code implementation of the website and the model is available here: [https://github.com/lcuvelli/master\\_thesis\\_dreasy](https://github.com/lcuvelli/master_thesis_dreasy).

The software is a web-based application, this choice is explained in Section 3.2. In Section 3.3, we present Flask, a Python web framework used to simplify the development of our website. In Section 3.4, we present the structure of our application and briefly explain the interactions between the web server and the client browser. Finally, Section 3.5 presents the user journey, which is the typical steps a user would go through when designing a dryer. This section also highlights some aspects implemented to ensure a smooth user experience.

### 3.2 Choice between desktop and web application

The purpose of this work is to create an open-access software to design and implement a simple solar dryer in order to help small-scale farmers communities. To implement this software, we have the choice between creating a desktop application or a web applications. We have chosen to develop a web application. This section compares the advantages and disadvantages of both possibilities and explains our choice.

A desktop application is a computer program that runs locally on a computer. A desktop application has to be downloaded beforehand and does not require an internet connection. Alternatively, a web application is stored on a remote server. A web browser (e.g. Google Chrome, Safari) is required, and content is delivered to a local device through internet. Table 3.1 compares desktop applications and web applications on several aspects.

Overall, web applications present many advantages compared to desktop applications. In the end, technological choices are guided by one criterion: it has to be as simple as possible for the user. Web applications do not require any download nor configuration, whereas desktop apps do. Considering all these elements, we choose to develop a web-based application for the design and implementation of a simple solar dryer.



	Desktop applications	Web applications
Internet connection	(+) no internet connection required	(-) internet connection required
Accessibility	(-) accessible only on the device that downloaded the program	(+) accessible on any device with a web browser, no location constraint
Platform dependency	(-) need to be developed separately for different platform machines	(+) platform-independent
Updates	(-) any update has to be done on individual client machines separately	(+) update is only done on the server machine
Security	(+) more secure	(-) higher security risks as inherently designed to increase accessibility

Table 3.1: Comparison between desktop application and web application on several aspects.  
Adapted from [30]

### 3.3 Flask framework

The web application developed in the context of this thesis is intended for the *Codepo* (Cellule de Coopération au développement de l'École polytechnique de Bruxelles). The permanent team of *Codepo* is composed of professors, technicians, researchers and technical experts in agri-food and biomedical. In the future, it is likely that the Codepo team will work on the website to improve some of its aspects. Therefore, the construction of the website must be simple and understandable for someone who is not necessarily an IT expert. Typically, non-IT experts are more likely to know high-level programming languages. Compared to lower-level languages, high-level languages are easier to understand for humans because they use terms that are similar to English. Hence, we chose to develop our web application using Python because of its simple programming syntax and code readability.

A web framework provides tools, libraries and technologies that allow to build a web application easily. There exist many web framework in Python and the choice of one particular framework depends on the functionalities and key features provided. In the context of this work, we use Flask framework [31]. Flask is considered as a microframework because it is very light: the web development is simple, but expandable. Like many frameworks, Flask is open source. It is also very popular and well documented.

Flask uses Jinja2 as template engine [32]. A template engine allows to set a basic layout for pages and mention which elements change. Updates on common elements for all pages only have to be modified at one place and not on every pages, which helps to keep consistency between pages. In the HTML scripts, variable data can be inserted dynamically.

### 3.4 Structure of the application

The structure of the software follows one of the common folder/file structures of a Flask application. In our application, files are grouped by function. The structure of the application is presented and explained below.

```

dreasy/
|-- model/
|   |-- air_flow_rate.py
|   |-- drying_section.py
|   |-- heat_transfer_coefficient.py
|   |-- heating_section.py
|-- static/
|-- templates/
|   |-- about.html
|   |-- airflow.html
|   |-- contacts.html
|   |-- database.html
|   |-- dryerdimensions.html
|   |-- home.html
|   |-- nav.html
|-- main.py
|-- requirements.txt

```

The repository `dreasy/` is the root of the project. The repository `model/` contains all the Python files used for the numerical resolution of the design procedure (see Section 2.5). The repository `static/` contains static files (images). The repository `templates/` contains all the HTML pages of the website. The file `main.py` is the start point of the software and basically launches the app. The file `requirements.txt` is a list of the necessary Python libraries and versions required for the code to run correctly.

The HTML files manage the content that is displayed on each page of the website. The layout is handled using CSS and Bootstrap [33]. Bootstrap is an open-source CSS framework. In this case, it has been used to facilitate the creation of the navigation bar, the layout of the forms and button, and the alignments of images and text. Bootstrap also allows responsible design: the elements and their layout change according to the screen size. Hence, the site is displayed correctly on any screen size, including smartphones.

The communication between the browser and the web server is done through HTTP requests and responses (Fig. 3.1). In our web app, the user fills a form with all the data and submits it. Then, the data are sent to the server using the GET method, which appends the form data into the URL. The data are processed through the code inside the model folder. The web server sends a response to the browser, the page is reloaded and the processed data are displayed.

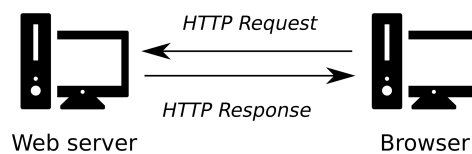


Figure 3.1: Client-server communication through HTTP [34]

## 3.5 User journey

This section aims to present the website developed and the typical steps a user would go through when designing a dryer. The name of the website is *Dreasy*, because drying is easy with Dreasy!

### 3.5.1 Home page

The first page of the website is the home page, presented on Fig. 3.2. The user can see brief information about the tunnel solar dryer. A navigation bar allows the user to navigate through the website. The tab « Design your solar dryer » and the button « Ready? Go to step 1 » lead to the same page, the first step of the design procedure.

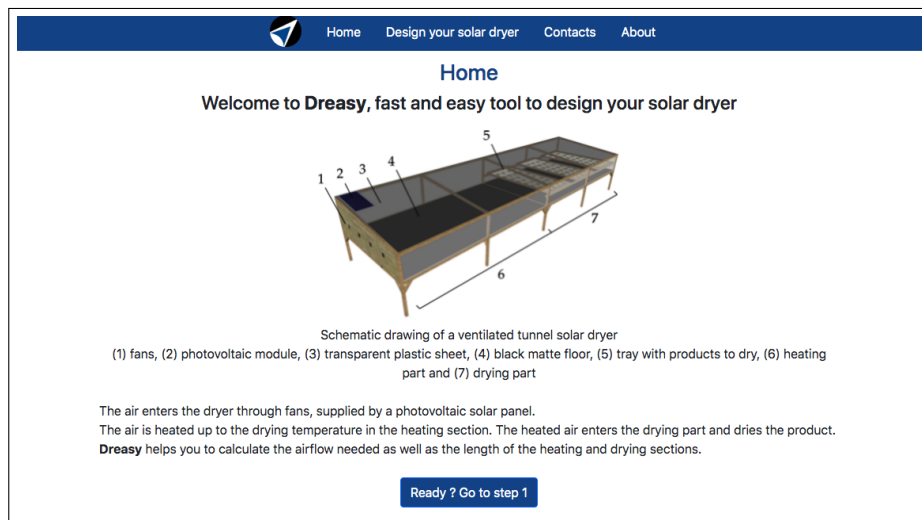


Figure 3.2: Home page of *Dreasy*

### 3.5.2 Design your solar dryer page

#### a) Ventilation system

The first step of the design procedure is to design the ventilation system by calculating the minimal air flow rate required inside the dryer. The user is invited to insert climatic data and product specifications. The user is informed that the drying time and the drying temperature highly influence the design procedure. (Fig. 3.3). In the case the user does not have access to these parameters, our database is available (Fig. 3.4).


Figure 3.3: Calculating the air flow rate required, the user is invited to enter climatic data and product specifications

Database - Drying time for fruits at different drying temperature and thicknesses						
Fruit	Initial humidity (d.b, kg water/kg dry product)	Thickness (mm)	Drying time (h) at temperature T			
			T = 40 °C	T = 50 °C	T = 60 °C	T = 70 °C
Apple	5.2	4.0	5.3	4.5	3.9	3.4
		6.0	8.9	7.6	6.6	5.7
Banana	3.3	4.0	9.3	8.0	6.9	6.0
		6.0	15.8	13.5	11.7	10.2
Mango	5.0	4.0	6.0	5.5	5.1	4.7
		6.0	10.1	9.3	8.6	8.0
Papaya	7.5	4.0	6.1	5.2	4.6	4.0
		6.0	10.3	8.9	7.7	6.8
Pineapple	6.0	4.0	7.9	7.0	6.3	5.7
		6.0	13.3	11.8	10.6	9.6

Figure 3.4: Database of the drying time for different dryer fruits at different drying temperature and slice thicknesses

To ensure the design algorithm works properly, conditions are imposed on user inputs. First, all values entered have to be numerical. Second, the value of some variables has to be inside a certain range (e.g. a relative humidity, expressed in percentage, is positive and cannot exceed 100). If the user enters a value which is not inside the value range defined, the website does not allow the user to send the form. Finally, some variables have an extra condition that needs to be fulfilled to make sure that values entered by the user are coherent. For example, the final moisture content of the product has to be lower than its initial moisture content. In the case the value range is respected but the extra condition is not, a warning message appears on the webpage when the user clicks on the button « Compute ». Even though some entries of the form are invalid, all values entered are kept in memory so that the user does not have to re-enter them all. Appendix B details range values and extra conditions for the different user inputs.

Fig. 3.5 illustrates warnings messages. The user has tried to enter a negative value for the mass of product to dry. The user is informed that the value entered has to be higher than 0. In this case, the message is displayed in French because it is a browser default message. The layout depends on the browser, and the language depends on the settings of the user. In addition, the user had previously entered a drying temperature lower than the mean ambient temperature of the air, which is not coherent because it means the dryer would have to cool the air. A warning message appears below the form, explaining clearly the problem to the user. The warning messages layout and content do not depend on the browser.


[Home](#)
[Design your solar dryer](#)
[Contacts](#)
[About](#)

### Step 1: Calculating minimal airflow for dryer

Once the minimal airflow for the dryer has been calculated, go to step 2

**Climatic data :**

Ambient relative humidity: ( $RH_{amb}$ ):  %

Ambient temperature: ( $T_{amb}$ ):  °C

**Specifications :**

Mass of product to dry: ( $M_0$ ):  kg

Initial moisture of products: ( $X_0$ ):  kg dry product

Final moisture of products: ( $X_f$ ):  kg dry product

Drying time: ( $t_d$ ):  h

Drying temperature: ( $T_d$ ):  °C

**Information**

The drying time ( $t_d$ ) and the drying temperature ( $T_d$ ) depend on the type of product and the thickness of the slices. Their value highly influence the dimensions of the dryer. Those values have to be coherent. In the case you are not sure about those values, check our [database](#)

Please fill all attributes.

Warning: Ambient temperature ( $T_{amb}$ ) should be **lower** than drying temperature ( $T_d$ ).

Figure 3.5: Example of warnings appearing when the user enters incoherent values


Once the user has entered all values correctly and press the button to send the form, the server calculates the air flow rate required to meet user requirements. The results are almost instantly displayed on the page (Fig. 3.6). The total mass of water to evaporate and the air flow rate, expressed in  $\text{m}^3/\text{h}$  are shown. There exists a multitude of possibilities to achieve a specific air flow rate. As mentioned before, a large fan in the middle of the entrance does not provide uniform ventilation, therefore we strongly advice the user to use smaller multiple fans. We give the example of a DC axial fan delivering  $20 \text{ m}^3/\text{h}$  from *RC Components*, and a link to this specific fan is given. In addition, we estimate the number of fans needed and the total cost for the user. The total power consumption is given and a link to solar pannels is given. The user is invited to go the the next step, through the button « Go to step 2 ».

Mass of water to evaporate is 8.6 kg.  
Your air flow rate should be : **100.0  $\text{m}^3/\text{h}$**

[Go to step 2](#)

To achieve this air flow, we strongly advice you to use multiple fans.  
⚠️ A large fan in the middle of the entrance does not provide uniform ventilation.

RS Components sells axial fans [here](#)



DC Axial Fan, Sunon, 12 V dc from RS Components

[This](#) fan has an airflow of  $20 \text{ m}^3/\text{h}$  and costs € 8.78  
Using this fan, you would need 5 fans for a total cost of € 43.9  
Such a small fan has a power consumption of 1.32 Watts  
Hence, the total power consumption of 5 fans is 6.6 Watts In order to deliver a constant flow rate, we recommend you to use a solar panel delivering at least twice this power. See [solar\\_panel](#)

Figure 3.6: Ventilation system information are displayed to the user

### b) Length of the heating and drying zones

The second and last step of the design procedure is to determine the lengths of the heating and drying zone. The user sees a page similar to the previous one, and he is asked to enter new data. Data entered previously as well as the air flow rate calculated at the step before are displayed (Fig. 3.7). However, these parameters are in read-only and the user is not allowed to modify them. This ensures that the air flow rate and the dimensions of the solar dryer are calculated for the same scope statement. Once the data are entered, the user sends the form through a button. The user is informed that computation might take a few minutes and the page should not be reloaded.

Home Design your solar dryer Contacts About

**Step 2: Calculating dimensions of the solar dryer**

[Go back to step 1](#)

**Climatic data :**

Diurnal direct and diffuse solar radiation flux ( $S_m$ ): [ ]  $\text{W/m}^2$

Diurnal atmospheric infrared radiation flux ( $I_{\text{atm}}$ ): [ ]  $\text{W/m}^2$

Ambient temperature ( $T_{\text{amb}}$ ): 30,0  $^{\circ}\text{C}$

Ambient relative humidity ( $RH_{\text{amb}}$ ): 70,0 %

Time of sunrise ( $t_{\text{rise}}$ ): [ ] h

Time of sunset ( $t_{\text{set}}$ ): [ ] h

**Specifications :**

Drying time ( $t_d$ ): 6,5 h

Drying temperature ( $T_d$ ): 60,0  $^{\circ}\text{C}$

Air flow rate ( $Q$ ): 100,0  $\text{m}^3/\text{h}$

Mass of product to dry ( $M_0$ ): 10,0 kg

Initial moisture of products ( $X_0$ ): 7,0 kg water/kg dry product

Final moisture of products ( $X_f$ ): 0,1 kg water/kg dry product

Reduction factor ( $k$ ): 0,85 (depends of plastic and wood structure)

Figure 3.7: Calculating the lengths of the heating and drying zone. Parameters entered previously are displayed but the user is not allowed to change them at this stage

Once the lengths have been calculated, the result is displayed below the page (Fig. 3.8). The starting time, the length of the heating section and the length of the drying section are displayed. Since we put a certain tolerance on the value of  $T_d$ , we also display the mean temperature achieved at the end of the heating section. A schematic of the flow cross section is also shown.

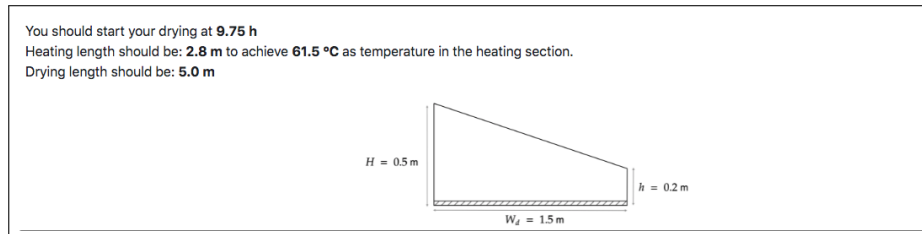


Figure 3.8: Starting time and lengths of the heating and drying sections are displayed. A schematic flow cross section with the dimensions is also displayed

### 3.5.3 Contacts page

The contact page lists the names and the email addresses of the persons who have contributed to this project so far. Hence, any user is able to contact us to ask questions about the project or to give us feedback.

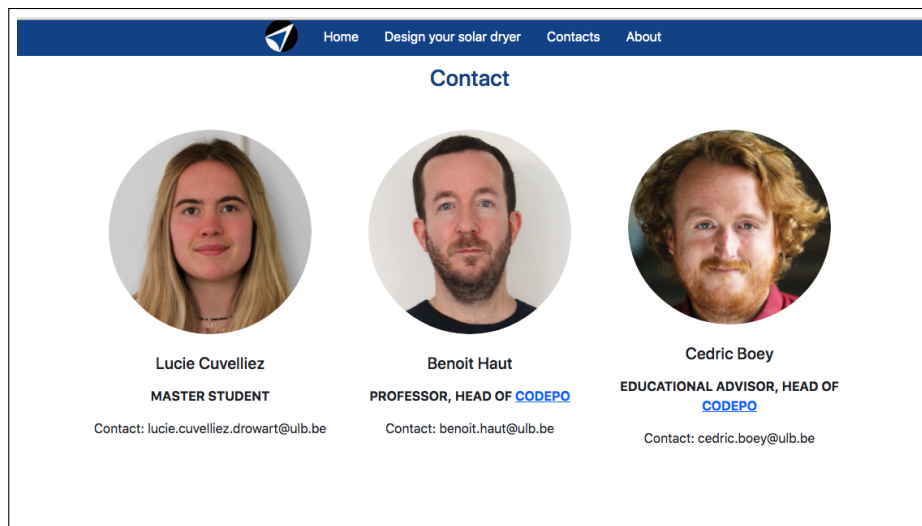


Figure 3.9: Contacts page

### 3.5.4 About page

The about page contains information about the project. It gives to the user some more information about the project and it also states that the website has been created in the context of a master thesis project. In addition, it contains this document.

## 3.6 Web hosting

We use the free version of the Google Cloud web hosting to host our website. The free version has limited capacity, but this solution is easy and already allows us to share our website. The website is available at: <https://dreasy-ulb.nw.r.appspot.com/> In the future, we would like to host the website on one of the ULB servers, but this is not yet possible because Python is not offered as a solution on the web hosting servers of ULB.

## Chapter 4

# Future work

### 4.1 Introduction

Although this thesis fulfills the objectives stated in Section 1.2 (i.e. design and development of an open-access software to design a solar dryer), further work is certainly required to improve various aspects of our work. Different improvements and experiments have been left for the future due to lack of time or current circumstances (i.e. experiments on the field require to travel to developing countries). Future work concerns deeper analysis of the model and proposals to improve the user journey on the website. This chapter presents the improvements considered as a priority. It is divided in two sections. The first section discusses further tests and analysis regarding the model. The second section suggests improvements regarding the website.

### 4.2 Model

#### 4.2.1 Experimental tests

Our design procedure is based on several assumptions and approximations. In order to evaluate the validity of our model, the theoretical results obtained should be checked on the field. More precisely, the temperature of the air at the end of the heating section  $T_{\text{air}}(t, z = L_H)$  and the temperature of the air at the end of the drying section  $T_{\text{air}}(t, z = L_D)$  should be monitored during the drying time and compared with theoretical results. In addition, the relative humidity at the end of the drying section should also be measured, to verify it respects the design conditions. Experimental tests are needed to estimate the impact of any differences between the theoretical model and reality.

#### 4.2.2 Sensitivity analysis of the parameters

The design procedure is inevitably sensitive to the values of the parameters that are introduced. In the future, a sensitivity analysis should be conducted on the different input parameters (initial moisture content of the product, mass to be dried, ...). The results could help to improve the model and to guide the user on the accuracy required for each parameter. Indeed, the values that the user enters are sometimes approximate, for example because data available in the literature do not reflect reality or because measurements have not been made meticulously. If the design procedure is highly sensitive to one parameter, then we could indicate to the user he needs to be cautious because this value has to be precise up to a certain factor. In the case a slight value change in one parameter does not influence significantly the design procedure, then we could indicate to the user that an approximation of the parameter is good enough. To take it a step further, this could also help the user that is not satisfied with the results obtained. For example, the user may have obtained a drying section of 8 meters, but is not satisfied with this length, judging it is too long. Our website could indicate what impact the variations of a parameter have on this length.

## 4.3 Website

### 4.3.1 Explanations and resources for the input parameters

The values of the input parameters are crucial for the design procedure. We already mention it to the user regarding the drying time and drying temperature, and we give their values for different fruits according to their thickness. For the other parameters, we do not explicitly mention what they are nor typical value ranges. While the name of a parameter could be enough for some users to understand what it represents, it might not be the case for every user. In any case, to avoid any confusion, it should be mentioned for every parameter what it refers to (for example, through an ephemeral informative window displayed when the mouse goes over this parameter). In addition, it would ease the user journey to give resources (e.g. tables, links) where the values of certain parameters are available and known to be accurate. In a more advanced version of this feature, the user could select some parameters and the others would be auto-filled or at least suggested. For example, the user could select the product to be dried through a drop-down menu, as well as the thickness of the slices and the drying temperature, and the website would automatically display the drying time. Similarly, the user could select a country and a period of the year and the website would display the relative climatic data.

### 4.3.2 User session

The current version of the website does not keep track of the outputs of the design procedure. We believe it would be useful for a user to be able to access previous results he has obtained. This can be easily implemented using an authentication system. When entering the website, a user would have the choice between create an account or continue as an unauthenticated user (i.e a guest). The account would offer the possibility to see the parameters and the outputs of design procedures previously done. This would allow the user to compare results with different input parameters.



## Chapter 5

# Conclusions

In this thesis, we addressed the problem of non-industrial solar drying in developing countries. We have created a website to design and implement a simple solar dryer to help small-scale farmers communities. More precisely, our design procedure allows to determine the air flow rate and the lengths of the heating and drying sections of a tunnel solar dryer operating in mix mode with forced convection. The design procedure is based on the one proposed by Talbot et al. [6] with some improvements. One of the main contributions of our work their work is to model the drying rate as a function of time and temperature, where it was previously considered as constant. The design procedure ensures that the drying temperature is on average constant, and that the drying is homogeneous. The air flow rate and the lengths of the heating and drying section are determined by solving energy and mass balance equations. Future work should include field experiments to validate the model and sensitivity analyses on the input parameters. Our website allows a user to design a dryer based on specifications. It is easy to use, and users do not necessarily need to have drying expertise. The website is based on the Flask framework and is currently hosted on the Google Cloud Platform. It is built in such a way that it can be used on any platforms: laptop, tablet and smartphones. The current version of the website performs as expected but in the future, we suggest to implement several features in order to ease the user journey. This includes adding information and resources regarding the different input parameters (mass to be dried, moisture content of the product, ...) and creating an authentication systems for users to save their results..

## Appendix A

# Drying time of different fruits for several slice thicknesses and drying temperatures

Fruit	Initial humidity (d.b, kg water/kg dry product)	Thickness (mm)	Drying time (h) for drying temperature $T$			
			$T = 40\text{ }^{\circ}\text{C}$	$T = 50\text{ }^{\circ}\text{C}$	$T = 60\text{ }^{\circ}\text{C}$	$T = 70\text{ }^{\circ}\text{C}$
Apple	5.2	4.0	5.3	4.5	3.9	3.4
		6.0	8.9	7.6	6.6	5.7
Banana	3.3	4.0	9.3	8.0	6.9	6.0
		6.0	15.8	13.5	11.7	10.2
Mango	5.0	4.0	6.0	5.5	5.1	4.7
		6.0	10.1	9.3	8.6	8.0
Papaya	7.5	4.0	6.1	5.2	4.6	4.0
		6.0	10.3	8.9	7.7	6.8
Pineapple	6.0	4.0	7.9	7.0	6.3	5.7
		6.0	13.3	11.8	10.6	9.6

Table A.1: Drying time of different fruits for several slice thicknesses and drying temperatures, obtained experimentally. Products are dried from their initial humidity to a final humidity of 0.05 kg water/kg dry product.

## Appendix B

# Conditions on user inputs in the website

Parameter	Value range	Extra condition
$I_{\text{atm}}$ , mean diurnal atmospheric infrared radiation flux ( $\text{W}/\text{m}^2$ )	$> 0$	–
$\text{RH}_{\text{amb}}$ , mean diurnal ambient air relative humidity (%)	$[0, 100]$	–
$S_{\text{atm}}$ , mean diurnal direct and diffuse solar radiation flux ( $\text{W}/\text{m}^2$ )	$> 0$	–
$T_{\text{amb}}$ , mean diurnal ambient temperature ( $^{\circ}\text{C}$ )	$[0, 50]$	–
$t_{\text{rise}}$ , sunrise time (h)	$[0, 24]$	–
$t_{\text{set}}$ , sunset time (h)	$[0, 24]$	$t_{\text{set}} \leq t_{\text{rise}}$
$M_0$ , mass of product to dry (kg)	$> 0$	–
$T_d$ , drying temperature ( $^{\circ}\text{C}$ )	$[0, 100]$	$T_d \geq T_{\text{amb}}$
$t_d$ , drying time (h)	$]0, 24]$	$t_d \leq t_{\text{set}} - t_{\text{rise}}$
$X_0$ , initial moisture content of product (kg water/kg dry product)	$> 0$	–
$X_f$ , final moisture content of product (kg water/kg dry product)	$> 0$	$X_f < X_0$

Table B.1: Conditions on user inputs in the website

If the user enters a value which is not inside the value range, the website does not allow the user to send the form. In the case the value range is respected but the extra condition is not, a warning message appears on the webpage when it is reloaded.

# Bibliography

- [1] L. Kivirist. *The Benefits of Drying Food*. Hobby Farms. Jan. 18, 2016. URL: <https://www.hobbyfarms.com/the-benefits-of-drying-food/> (visited on 04/26/2021).
- [2] B. Axtell and T. Swetman. *Small-scale Drying Technologies, Practical Action*. <http://hdl.handle.net/11283/314540>. United Kingdom. This fact sheet describes improved drying systems that are suitable for use by small-scale producers. 2003.
- [3] M. Owureku-Asare et al. "Physicochemical and Nutritional Characteristics of Solar and Sun-dried Tomato Powder". In: *Journal of Food Research* 7 (Sept. 2018), p. 1. DOI: 10.5539/jfr.v7n6p1.
- [4] M. G. Green and D. Schwarz. *Solar Drying Technology for Food Preservation*. 2002.
- [5] D. G. Mercer. "Solar Drying in Developing Countries: Possibilities and Pitfalls". In: *Using Food Science and Technology to Improve Nutrition and Promote National Development: Selected Case Studies*. International Union of Food Science & Technology (IUFoST), 2008. Chap. 4. ISBN: 978-0-9810247-0-7.
- [6] P. Talbot et al. "Ventilated tunnel solar dryers for small-scale farmers communities: Theoretical and practical aspects". In: *Drying Technology* 34.10 (2016), pp. 1162–1174. DOI: 10.1080/07373937.2015.1121395.
- [7] E. Morm et al. "Experimental Characterization of the Drying of Kampot Red Pepper (*Piper nigrum* L.)". In: *Foods* 9.11 (Oct. 2020), p. 1532. DOI: 10.3390/foods9111532. URL: <https://doi.org/10.3390/foods9111532>.
- [8] D. I. Onwude et al. "Modeling the Thin-Layer Drying of Fruits and Vegetables: A Review". In: *Comprehensive Reviews in Food Science and Food Safety* 15.3 (Feb. 2016), pp. 599–618. DOI: 10.1111/1541-4337.12196. URL: <https://doi.org/10.1111/1541-4337.12196>.
- [9] C. Heilporn. "Contribution au développement d'une nouvelle technologie de séchage solaire. Application à la mangue". PhD thesis. Université libre de Bruxelles, 2013.
- [10] A. Tiwari. "A Review on Solar Drying of Agricultural Produce". In: *Journal of Food Processing and Technology* 7 (2016), pp. 1–12. DOI: 10.4172/2157-7110.1000623.
- [11] M. Augustus Leon, S. Kumar and S.C Bhattacharya. "A comprehensive procedure for performance evaluation of solar food dryers". In: *Renewable and Sustainable Energy Reviews* 6.4 (Aug. 2002), pp. 367–393. DOI: 10.1016/S1364-0321(02)00005-9. URL: [https://doi.org/10.1016/S1364-0321\(02\)00005-9](https://doi.org/10.1016/S1364-0321(02)00005-9).
- [12] P. Vanderhulst. *Solar energy: small-scale applications in developing countries*. OCLC: 43770590. Amsterdam: TOOL Foundation, 1990. ISBN: 978-90-70857-19-6.
- [13] B. Norton. "3.17 - Industrial and Agricultural Applications of Solar Heat". In: *Comprehensive Renewable Energy*. Ed. by Ali Sayigh. Oxford: Elsevier, 2012, pp. 567–594. ISBN: 978-0-08-087873-7. DOI: <https://doi.org/10.1016/B978-0-08-087872-0.00317-6>. URL: <https://www.sciencedirect.com/science/article/pii/B9780080878720003176>.
- [14] A. O. Dissa, H. Desmorieux, J. Bathiebo and J. Koulidiati. "A comparative study of direct and indirect solar drying of mango". In: *Global Journal of Pure and Applied Sciences* 17.3 (2011). Number: 3, pp. 273–294. ISSN: 1118-0579. DOI: 10.4314/gjpas.v17i3. URL: <https://www.ajol.info/index.php/gjpas/article/view/78801> (visited on 05/09/2021).
- [15] E. Ayua et al. "Comparison of a mixed modes solar dryer to a direct mode solar dryer for African indigenous vegetable and chili processing". In: *Journal of Food Processing and Preservation* 41.6 (2017), e13216. DOI: <https://doi.org/10.1111/jfpp.13216>. URL: <https://ifst.onlinelibrary.wiley.com/doi/abs/10.1111/jfpp.13216>.

- [16] K. Limpai boon and S. Wiriyaumpaiwong. “Drying Kinetics of Steamed Glutinous Rice with a Free Convective Solar Dryer”. In: *Walailak Journal of Science and Technology* 6 (June 2009). DOI: 10.2004/wjst.v6i2.61.
- [17] B. Bukola and O. Ayoola. “Performance Evaluation of a Mixed-Mode Solar Dryer”. In: *AU Journal of Technology* 11 (Apr. 2008), pp. 225–231.
- [18] Y. M. Jibhakate, Dr. A. C. Waghmare and Dr. S. K. Choudhary. “Performance Evaluation of Solar Tunnel Dryer for Drying Red Chilli using Taguchi L27 Orthogonal Array”. In: 2016.
- [19] *FAOclim 2.0 software*. Software Informer. URL: <https://faoclim.software.informer.com/2.0/>. Accessed May 10, 2021.
- [20] *SunEarthTools.com*. Outils pour les consommateurs et les concepteurs de l’énergie solaire. URL: <https://www.sunearthtools.com/>. Accessed May 10, 2021.
- [21] *Weatherbase*. URL: <http://www.weatherbase.com/>. Accessed May 10, 2021.
- [22] D. Mercer. *An Introduction to the Dehydration and Drying of Fruits and Vegetables*. Oct. 2014. ISBN: 978-0-88955-621-8.
- [23] W. Canet. “Determination of the Moisture Content of Some Fruits and Vegetables by Microwave Heating”. In: *Journal of Microwave Power and Electromagnetic Energy* 23.4 (Jan. 1988), pp. 231–235. DOI: 10.1080/08327823.1988.11688062. URL: <https://doi.org/10.1080/08327823.1988.11688062>.
- [24] J. Carvill. “3 - Thermodynamics and heat transfer”. In: *Mechanical Engineer’s Data Handbook*. Ed. by J. Carvill. Oxford: Butterworth-Heinemann, 1993, pp. 102–145. ISBN: 978-0-08-051135-1. DOI: <https://doi.org/10.1016/B978-0-08-051135-1.50008-X>. URL: <https://www.sciencedirect.com/science/article/pii/B978008051135150008X>.
- [25] G. Kell. “Density, thermal expansivity, and compressibility of liquid water from 0.deg. to 150.deg.. Correlations and tables for atmospheric pressure and saturation reviewed and expressed on 1968 temperature scale”. In: *Journal of Chemical Engineering Data* 20 (1975), pp. 97–105.
- [26] T. L. Bergman, D. P. DeWitt, F. Incropera and A.S. Lavine, ed. *Introduction to heat transfer*. 6th ed. OCLC: ocn739732416. Hoboken, NJ: Wiley, 2011. 960 pp. ISBN: 978-0-470-50196-2.
- [27] Y. Yener, S. Kakac, and A. Pramuanjaroenkij. *Convective Heat Transfer (3rd ed.)* CRC Press, 2013. DOI: <https://doi.org/10.1201/b16194>.
- [28] E. Mirzaee, S. Rafiee, A. Keyhani and Z. Emam-Djomeh. “Determining of moisture diffusivity and activation energy in drying of apricots”. In: *Research in Agricultural Engineering* 55.No. 3 (Sept. 2009), pp. 114–120. DOI: 10.17221/8/2009-rae. URL: <https://doi.org/10.17221/8/2009-rae>.
- [29] C. Herman, L. Spreutels, N. Turomzsa, E. Mayumi Konagano and B. Haut. “Convective drying of fermented Amazonian cocoa beans (Theobroma cacao var. Forasteiro). Experiments and mathematical modeling”. In: *Food and Bioproducts Processing* 108 (Mar. 2018), pp. 81–94. DOI: 10.1016/j.fbp.2018.01.002. URL: <https://doi.org/10.1016/j.fbp.2018.01.002>.
- [30] D. Bychkov. *Desktop vs. Web Applications: A Deeper Look and Comparison*. Segue Technologies. June 7, 2013. URL: <https://www.seguetech.com/desktop-vs-web-applications/>. Accessed May 18, 2021.
- [31] *Welcome to Flask — Flask Documentation (2.0.x)*. URL: <https://flask.palletsprojects.com/en/2.0.x/>. Accessed May 18, 2021.
- [32] *Jinja — Jinja Documentation (3.0.x)*. URL: <https://jinja.palletsprojects.com/en/3.0.x/>. Accessed May 18, 2021.
- [33] J. Thornton, M. Otto and contributors. *Bootstrap*. URL: <https://getbootstrap.com/>. Accessed May 19, 2021.
- [34] M. Dorman. *Chapter 5 Web Servers / Introduction to Web Mapping*. CRC Press, 2020. URL: <https://geobgu.xyz/web-mapping/web-servers-1.html>.